INL/ RPT-22-66120
Revision 0

Preconceptual Design of Irradiated Fuel Salt Management System

February 2022

Semin Joo

Idaho National Laboratory

INL is a U.S. Department of Energy National Laboratory
operated by Battelle Energy Alliance, LLC

INL/RPT-22-66120
Revision 0

Preconceptual Design of Irradiated Fuel Salt Management System

Semin Joo

February 2022

Idaho National Laboratory
Idaho Falls, Idaho 83415

http://www.inl.gov

Prepared for the
U.S. Department of Energy
Office of Nuclear Energy
Under DOE Idaho Operations Office
Contract DE-AC07-05ID14517

Page intentionally left blank

ABSTRACT

The National Reactor Innovation Center was established by the U.S. Department of Energy to accelerate the demonstration and deployment of advanced nuclear reactors. To meet this mission, the National Reactor Innovation Center has developed the Laboratory for Operations and Testing in the U.S. (LOTUS) to support the first fast-spectrum molten salt reactor demonstration. The goal of this research is to understand the system requirements that may be applied to a molten salt reactor experiment in the LOTUS test bed and to perform systems analyses and preconceptual development of a storage container for the management of the irradiated molten salt fuel. This study proposes a set of irradiated fuel salt management processes for the molten salt reactor, from defueling to storage or disposal. For that, the historic Molten Salt Reactor Experiment (MSRE) at Oak Ridge National Laboratory has served as a crucial source of data for a mock application.

This paper proposes a potential geometry for storing irradiated fuel salt based on MSRE data and the Monte Carlo N-Particle radiation transport code. The geometry was analyzed for criticality safety under abnormal situations, such as water ingress and interaction between containers. Based on the determined configuration of the storage system, the decay heat produced from the irradiated fuel salts was calculated to provide a reasonable time scale of the dormancy period. Using the same geometry assumed above, the neutron and gamma dose rates from the irradiated fuel salt at the end of the dormancy period were estimated, which will be useful for understanding the handling and radiation protection requirements for handling the irradiated fuel salt.

Lastly, a reactor in the LOTUS test bed could use chloride-based fuel as opposed to the fluoride-based fuel used in MSRE. Thus, a literature study provided data to understand the similarities and differences between the characteristics of fluoride- and chloride-based salts in terms of salt chemistry, material characteristics, postirradiation behavior, neutronics, thermal hydraulics, and heat removal. This study, together with the proposed irradiated fuel salt management processes, preliminary criticality calculations, decay heat, and dose rate estimates, provides a strong basis for future investigation into the management of irradiated fuel salts generated during molten salt reactor technology demonstrations.

Page intentionally left blank

ACKNOWLEDGEMENTS

This work was supported by Nuclear Global Internship Program through the Korea Nuclear International Cooperation Foundation funded by the South Korean Ministry of Science and Information and Communication Technology.

This study could not have been finished without my mentors Evans Kitcher and Kristina Spencer. Their guidance and advice carried me through all the stages of writing this report. Without their detailed and critical reviews on the draft, this report could not have been published.

Also, I would like to give special thanks to my supervisor Stanley Andrew Orrell for arranging this project and giving me continuous support.

Page intentionally left blank

CONTENTS

FIGURES

TABLES

Page intentionally left blank

ACRONYMS

kWt	kilowatts thermal
LOTUS	Laboratory for Operations and Testing in the U.S.
MCNP	Monte Carlo N-Particle
MSR	molten salt reactor
MSRE	Molten Salt Reactor Experiment
MWt	megawatts thermal
ORNL	Oak Ridge National Laboratory
USL	upper subcritical limit

Page intentionally left blank

Preconceptual Design of Irradiated Fuel Salt Management System

1. INRODUCTION

1.1 Background

In 2019, the National Reactor Innovation Center was established by the U.S. Department of Energy to accelerate the demonstration and deployment of advanced nuclear reactors. To meet this mission, the National Reactor Innovation Center is developing two reactor test beds to perform critical advanced reactor experiments by the end of 2025. They are the Demonstration and Operation of Microreactor Experiments and the Laboratory for Operations and Testing in the U.S. (LOTUS) test beds. These test beds are intended to demonstrate the life cycle of new reactors, from construction to storage or disposal. The Demonstration and Operation of Microreactor Experiments test bed will support reactors with thermal outputs under 20 MWt using low-enriched uranium. Meanwhile, the LOTUS test bed will support reactors with thermal outputs under 500 kWt and fuels are highly enriched uranium or Pu-based fuels. This test bed will at Idaho National Laboratory and is the proposed host for a molten chloride fast reactor in a collaboration between TerraPower, Idaho National Laboratory, and Southern Company.[1] If successful, this will be the world's first fast-spectrum, salt-fueled nuclear reactor.

1.2 Project Description

In preparation for hosting a molten salt reactor (MSR) in LOTUS, the management plans for decommissioning, waste management, and irradiated fuel salt management must be established. These plans are in a preconceptual phase. The work presented here proposes an irradiated fuel salt management process for the reactor with an accompanying set of high-level requirements. For this work, the historic Molten Salt Reactor Experiment (MSRE) at Oak Ridge National Laboratory (ORNL) has served as a crucial source of data.

1.2.1 Goals

- Develop preconceptual systems requirements for handling highly enriched uranium–based molten salt fuel in the LOTUS test bed
- Perform systems analyses and preconceptual development of a storage container for the irradiated fuel salt and flush salts
- Evaluate the design concept for its applicability to molten chloride systems

1.2.2 Assumptions

- A storage container designed to store irradiated fuel salt at the end of the experimental timeframe
- Criticality analyses of the fresh fuel salt composition, assuming that the fresh fuel is more reactive than the irradiated fuel salt

1.2.3 Detailed Tasks

- Compare fluoride- and chloride-based salts in terms of heat transfer, corrosion chemistry, neutronics, and material characteristics
- Study the MSRE case and predict what changes would occur when the system changes into a chloride-based system
- Write a set of high-level descriptions for each part of the irradiated fuel salt management process, starting with defueling and ending with storage

- Identify credible abnormal situations that could happen to the system
- Find the requirements that would enable the system to safely operate at normal or abnormal conditions

2. BACKGROUND – MOLTEN SALT REACTOR EXPERIMENT

2.1 Overview and Operational History

The historic MSRE at ORNL has served as a crucial source of data for developing MSR designs as the world's second MSR in operation. It was an 8-MW-class experimental reactor that operated for 4 years, from 1965 to 1969.[2] Its fuel salt was based on LiF-BeF_2-ZrF_4, in which fissile material, UF_4, was dissolved. It was initially loaded with 218 kg of uranium, of which 30 wt% was U-235 and 70% was U-238. Later, MSRE was refueled with approximately 37 kg of uranium, consisting of 80 wt% of U-233 and 20 wt% of U-235.

After the reactor was shut down, the fuel salt inside the core was drained down to the two fuel drain tanks using gravity. Then, flush salts were circulated through the core to clean up the remaining fuel salts then drained down into a flush salt drain tank. The two fuel drain tanks and the flush salt drain tanks were collocated inside the drain tank cell (see Figure 2-1). Each fuel drain tank contained about 2,000 kg of fuel salts, and the flush salt drain tank contained about 4,000 kg of flush salts.

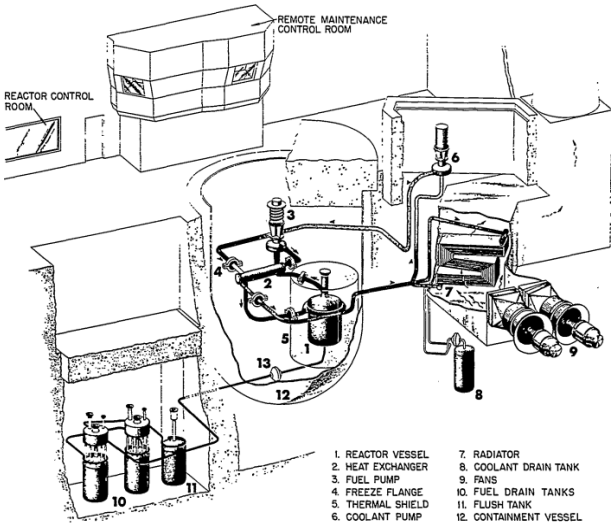

Figure 2-1. Schematic diagram of MSRE.[3]

After the salts were drained, MSRE required frequent and significant maintenance, mainly attributed to fluorine gas production. The irradiated fluoride salt generated free fluorine, and as the salts cooled, the free fluorine recombined to form fluorine gases. Further, the fluorine gases reacted with uranium to form uranium hexafluoride. To prevent these gases from filling the drain tank and increasing the pressure, MSRE needs periodic ventilation and maintenance.[4]

In 1994, a failure in one of the off-gas pipes connected to the drain tanks was discovered. Due to this failure, fluorine and uranium hexafluoride gases migrated to the off-gas system and the auxiliary charcoal beds that were built to trap gaseous fission products. The amount of deposited uranium on the charcoal beds was substantial, so ORNL performed interim corrective measures to prevent criticality. The first step, a so-called "Time-critical Removal Action," was performed in 1995, wherein ORNL controlled the nuclear criticality and installed a reactive gas removal system. In 1996, ORNL performed a "Non-time-critical Removal Action" to remove the uranium deposits and fluorine from the charcoal beds. The last step that the ORNL has planned is the "Remedial Action" to remove fuel and flush salts from the drain

tanks.[3] This action has not been completed yet, leaving the solidified salts inside the drain tanks.

2.2 Current Status (2021)

The decommissioning of MSRE is managed by URS CH2M Oak Ridge LLC (UCOR), a cleanup contractor for ORNL. According to UCOR, the 2021 status of MSRE can summarized as [5]:

- The salts are cooled and solidified into a monolithic mass.
- Uranium is present at less than 2.5 kg per tank.
- The radioactivity of fission and activation products is dominated by Cs-137 and Sr-90.
- The volatile fission products are not retained in the fuel but treated via an off-gas system.
- The actinide inventory is governed by U-232 and U-233 decay chains.
- The flush salt contains less than 2% of uranium and fission products.
- The shield blocks on the top of the drain tanks are replaced with maintenance shields to gain access to the drain tanks.
- The drain tank cell is an extremely high radiation area to work in (see Table 2-1).

Table 2-1. Radioactivity of MSRE drain tanks (2021).[5]

	Fuel Salt Drain Tank #1	Fuel Salt Drain Tank #2	Flush Salt Drain Tank
Radioactivity [Ci]	6,800	5,700	200

2.3 Decommissioning Challenges

There are two main reasons that make the MSRE decommissioning challenges distinct from other nuclear reactors. The first reason is because MSRE is a molten salt reactor. There are some inherent challenges that arise from being an MSR, such as fluorine generation, uncertainties in the long-term waste form, an absence of a regulatory framework on salt wastes, etc. [2] These challenges are also displayed in the MSRE case.

- Potential gas generation: Irradiated fluoride-based salts generate free fluorine. Free fluorine tends to readily recombine to form fluorine gas under 200. Also, fluorine gas can react with UF_4 to form UF_6, which easily migrates to other reactor components. Thus, fluoride-based MSRs require continuous ventilation, as happened with MSRE after operation.
- Uncertainties in the long-term waste form: Little research exists on MSR salt waste forms. This is not only because the current MSR research is focused on the front-end cycle but also because only two experimental MSRs have ever been operated. A disposition option based on the precise form, radioactivity, and heat generation of the salt wastes must be found before the next MSR is constructed.
- Absence of regulatory framework: Many U.S. companies are proposing new MSR concepts. However, the full regulatory framework that would help realize those designs is absent.

The second reason for the distinctive challenges is because of the unique characteristics of MSRE.

- First, MSRE is comprised of aging facilities and equipment. Since its shutdown in 1969, more than five decades have passed. During those 50 years, the harsh fluorine environment has increased the potential risk of a breach of the drain tanks. Additionally, the MSRE systems rely on a ventilation system design that is original to the facility for *safety-significant* functions. When MSRE was designed, the post-operation measures and plans were not set, making MSRE suboptimal for decommissioning.
- Second, MRSE has a challenging working environment due to hazardous conditions. As shown in Table 2-1, the drain tank cells are highly radioactive requiring multiple approaches to limiting exposure, such as personal protective equipment, special tools, portable maintenance shields, etc. That these efforts are needed today reflects that this MSRE was built at a time when the

regulatory framework allowed higher exposure limits.

- Lastly, the waste forms and disposition options for MSRE bear several uncertainties. The expected major waste streams are irradiated fuel salts, salt-contaminated components, U-laden charcoal, and lead.[6] Among them, the U-laden charcoal was produced from the unexpected migration of UF_6 due to a pipe failure. The question of how to dispose the U-laden charcoal needs to be answered, together with finding a disposition option for irradiated fuel salt wastes. For the fuel salt waste, MSRE salt wastes could be sent to the Waste Isolation Pilot Plant, a deep geological repository that only accepts transuranic wastes from defense programs. MSRE salt wastes satisfies the waste acceptance criteria of the Waste Isolation Pilot Plant, but whether the MSRE salts can be classified as defense wastes is still controversial.[5]

3. DESCRIPTION OF THE IRRADIATED FUEL MANAGEMENT PROCESS

3.1 Objectives

The irradiated fuel management of an MSR was designed to:

- Ensure the safe storage or disposal of radioactive salt wastes
- Fulfill the waste confidence principle, ensuring that there is a secure irradiated fuel salt management process after a reactor is shut down
- Develop a realistic irradiated fuel salt management process reflecting the current disposition options and techniques in the U.S.

3.2 Overview of the Process

3.2.1 Primary Actions

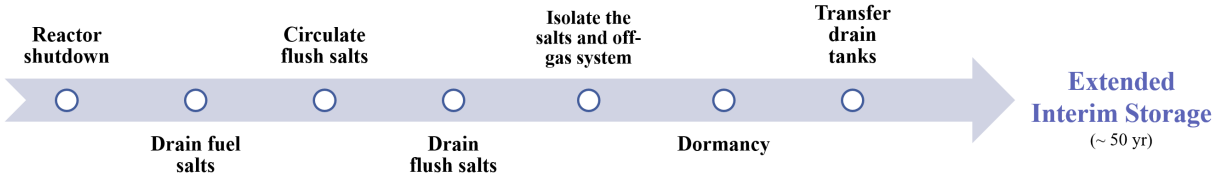

Figure 3-2. Flowchart of the primary actions for irradiated fuel management.

At the end of the experiment, the reactor will undergo a set of primary actions before the salt treatment process begins. First, the reactor should be completely shut down. Then, the fuel salts inside the reactor core will be drained through gravity into the fuel salt drain tanks. Subsequently, flush salts, i.e. molten salts that have the same composition as the fresh fuel salt without fissile materials, will be circulated through the reactor core to remove as much of the residual fuel salts as possible from the structural materials. After the flush is complete, the flush salt will also be drained into drain tanks.

The next step is to prepare for a dormancy period. Here, the irradiated fuel salt and contaminated flush salt inside the drain tanks and the off-gas system should be isolated from other reactor components. Note that the drain tanks and off-gas system should be connected so that hazardous gases, such as volatile fission products, hydrogen fluoride gas, or fluorine gases produced from the fuel salts, can be vented out and captured by the off-gas system. In this step, it is crucial to monitor and confirm that the hazardous gases are not migrating to other reactor components. Once the isolation of irradiated fuel salts and contaminated flush salts is confirmed, the entire reactor system moves on to the dormancy period. Here, the level of heat and radioactivity of the fuel salts is reduced until those levels are below the threshold where subsequent operations can begin. Note that the maintenance systems that maintain the drain tank vacuums and purge hazardous gases should be operating continuously during this period.

After the dormancy period, the level of heat and radioactivity would have dropped below the targeted level. Then, the irradiated fuel salts and contaminated flush salts can be transferred to other facilities for treatment. If the necessary treatment capabilities are not available, the irradiated fuel salts and contaminated flush salts will be transferred to an interim storage facility. This storage option will accommodate the irradiated fuel salts and contaminated flush salts for up to 50 years.

3.2.2 Irradiated Fuel Management Process

With salt treatment capabilities in place, the irradiated fuel salt and contaminated flush salt will be transported out from the interim storage facility to the salt treatment location. As shown below, the irradiated fuel salt will go to the fuel salt treatment location, while the contaminated flush salt will go to the flush salt treatment location to undergo different processes.

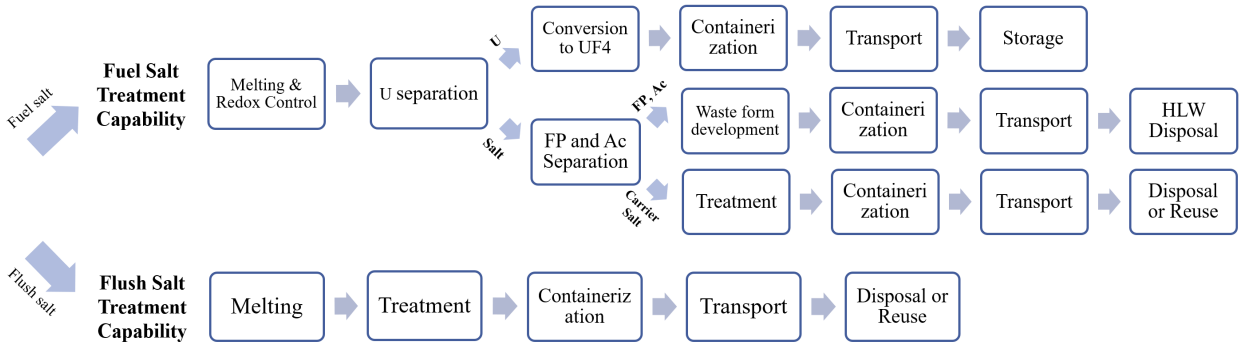

Figure 3-3. Flowchart of the irradiated fuel management process.

Irradiated Fuel Salt

The irradiated fuel salt will be melted to facilitate chemical control and salt transfer. Simultaneously, the melting salts require redox control. As the salts are melted, the fluorine gases generated makes the salt a strongly reducing environment. This facilitates uranium precipitation out of the fuel salt, which poses a criticality safety concern. Thus, redox control during the melting process is particularly important.

After the fuel salt is completely melted, the uranium will be separated from the salts. The extracted uranium will be subsequently converted into uranium tetrafluoride (UF_4), which is an appropriate form because of its high flexibility for reuse and low estimated costs.[7] Then, the converted uranium will be put into a container designed for storage. After which, the containers will be transported to the final storage site.

The remaining salts without uranium will then undergo a separation process. The fission products and actinides will be removed so that the volume of high-level wastes (HLW) is reduced. Salt wastes containing important fission products and actinides will likely be classified as HLW. The separated waste stream will be immobilized into a waste form that could be accepted at a designated HLW disposal facility. The HLW will be poured into encapsulation containers that meet the site criteria, sealed, solidified, and transported to the HLW disposal site.

The last waste stream left is the carrier salt, which is now absent of uranium, actinides, and important fission products. This carrier salt now has a low radioactivity and heat generation rate, so that, even without any additional separation of radionuclides, it will be classified as a low-level-waste (LLW). Hence, the carrier salt will be appropriately treated and transferred to salt storage containers. From here, the treatment options will be divided into two branches, depending on whether the final disposition option is disposal or reuse. Since the carrier salt should have almost the same composition as the fuel carrier salt, and since fabricating a new carrier salt requires high effort and costs, it might be preferable to reuse the carrier salt for other molten salt applications. However, the regulations related to reusing the salts are absent, and there are uncertainties in the performance of reused salts. Thus, this report does not determine the final disposition option for the carrier salt. Instead, the pros and cons of each option are laid out in Table 3-1.

Table 3-2. The pros and cons of LLW disposal vs. reusing the carrier salts.

	LLW Disposal	Reuse
Pros	Doesn't require new technology to reuse the carrier salt Simple, straightforward path If the salt wastes can be simply classified as LLW, they could be disposed at widely available LLW disposal facilities.	Reduces the future cost of fabricating new carrier salts (e.g., cost of Li-7 enrichment) Separated carrier salt can be directly put into facilities fabricating new fuel salt Since U, fission products, and actinides have been separated out from the salts, less treatment would be required to reuse the salts
Cons	Fabrication costs of carrier salts are too high to just dispose of the salt No regulations or facilities to dispose the salt wastes exist in the U.S.	Uncertainties exist: Will the salt still perform well after irradiation? What kinds of treatment processes are required for to reuse carrier fuel salts? No current regulations on salt reuse

If the carrier salts are going to be disposed of at a LLW disposal facility, the salts inside the container should be processed into a form that meets the waste acceptance criteria of an appointed LLW disposal facility. This treatment will include processes such as ensuring a solid waste form, compaction, immobilization, etc. After the treatment and containerization, the salt storage containers would be transported to the LLW disposal facility.

On the other hand, if the carrier salt is to be reused, it should be chemically or physically treated to recover its initial performance in terms of heat transfer, corrosion behavior, material characteristics, neutronics, etc. Treatment options and techniques will be informed by further studies on irradiated molten salts. If the treated salts are scheduled to be reused somewhere immediately, the containers will be sealed and transported to that site. If not, the containers will be stored temporarily at the reactor site, waiting for an upcoming demand.

Contaminated Flush Salt

The treatment processes for the contaminated flush salts are much simpler than those for the irradiated fuel salts. First, the flush salts should be heated and melted to facilitate chemical control and salt transfer. As the flush salts only contain a little uranium, criticality is assumed improbable during the melting process, thus redox control is not required. When the flush salts are completely molten, they will be transferred to salt storage containers. Similar to the carrier salt stream, the final disposition option is not clear here. It could be either disposed at an LLW disposal facility or be reused for other molten salt applications. If both carrier salts and flush salts are to be disposed, they are expected to be transferred to the same LLW disposal facility. But if both salts are to be reused, they will undergo similar treatment processes to recover their initial performances.

3.2.3 Proposed Irradiated Fuel Management Capabilities

Several capabilities are needed for salt management. Figure 3-3 shows the relationship of the capabilities in order to manage the irradiated fuel salt and other salt wastes generated as part of the decommissioning process.

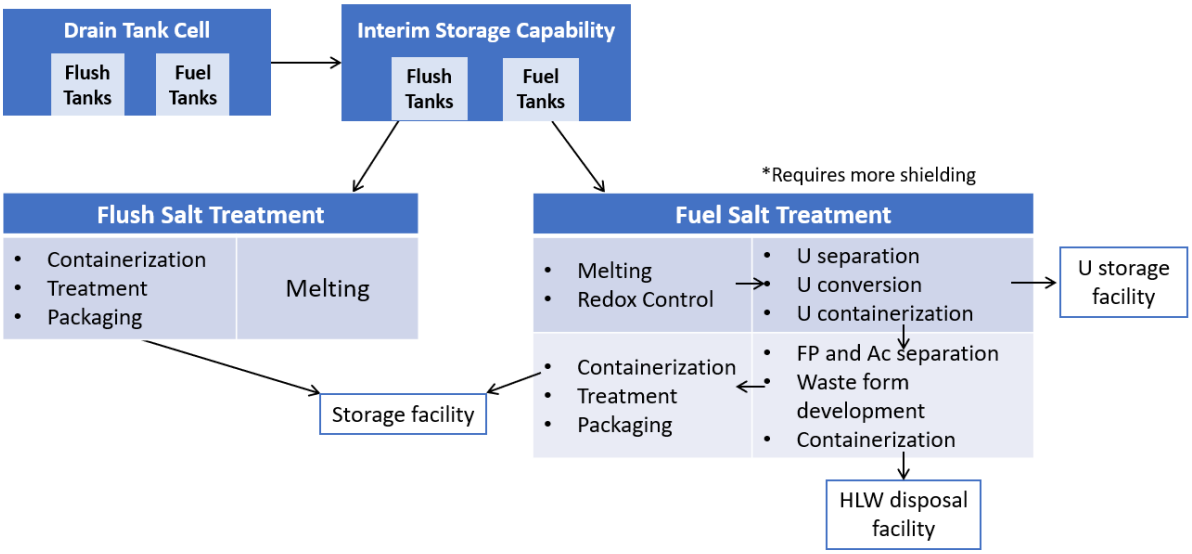

Figure 3-4. Proposed irradiated fuel management capabilities.

The drain tank cell, a part of the MSR facility, contains flush salt drain tanks and fuel salt drain tanks. The tank contents are transferred to irradiated fuel containers and flush salt containers. These containers are then transferred to the interim storage facility and stored until the salt treatment capabilities are available. The interim storage facility is expected to be operable for up to 50 years to give ample time to complete the process.

The fuel salt treatment capability is for processing the fuel salts. The presence of hazardous fission products and transuranic elements in the irradiated fuel salt requires more complex treatment and separation processes. Hence, the fuel salt treatment capability should be able to perform a wide variety of functions, such as melting and redox control, uranium handling, fission product and actinides handling, and carrier salt processing. Each of these will require specialized equipment to perform the treatment. For instance, uranium handling will require equipment that separates uranium from the salts, equipment to convert the separated uranium into a tetrafluoride form, and equipment for packing the uranium for storage.

Fuel salt treatment capabilities require a significant amount of shielding, due to the radiation field associated with the irradiated fuel salt. Meanwhile, the flush salt treatment capability will require relatively less shielding. The contaminated flush salts are expected to have almost the same composition as that of the original flush salt, reducing the necessity of thick shielding. This difference in shielding and handling requirements suggests that separating the two capabilities would reduce the overall costs involved, assuming costs are dominated by shielding requirements.

3.3 Description of Irradiated Fuel Management Processes

This section presents a description of each part of the irradiated fuel salt and contaminated flush salt management process proposed above. The requirements will include the purpose of each step, underlying assumptions, preconditions and postconditions, systems involved in the step, and the system interfaces. The requirements are organized in Table 3-2, 3-3, 3-4, 3-5, 3-6, and 3-7.

3.3.1 Primary Actions

Table 3-3. High-level requirements for primary actions.

1. Reactor Shutdown and Fuel Salt Drainage	
Purpose	• To stop the operation of the reactor and other reactor components, such as the heat exchanger and coolant pumps • To drain the fuel salt from the reactor core to the fuel salt drain tanks

	• To start the primary actions of the decommissioning process
Assumptions	The shutdown will be gradual, not an emergency occurring at accident situations. Thus, the burnup and fuel composition will resemble those of typical spent fuels.
Preconditions	The experiment or operation plan has terminated.
Systems involved	• Reactor core • Control rods • Decay heat removal system • Fuel salt drain tanks
Interface	Control-rod mechanism, decay heat removal system and reactor core, reactor core and fuel salt drain tanks
Break conditions	• Decay heat removal system operates • Heat exchanger stops electricity generation • No fuel movements • Subcritical and sufficient shutdown reactivity • As many fuel salts as possible moved to the fuel salt drain tank
Postconditions	Reactor is shut down, fuel salts are molten inside the fuel salt drain tanks
2. Transfer the Irradiated Fuel Salt	
Purpose	To transfer the irradiated fuel salt from the fuel salt drain tank to the irradiated fuel containers (nominally 36 containers) inside the drain tank cell to clear the reactor core
Assumptions	Each fuel salt drain tanks is so heavy (in the MSRE case, 4,000kg) and contains such a large amount of uranium that transporting them to the interim storage facility would be unrealistic. By dividing the fuel salts into multiple containers that are capable of transport and storage, further processes after the dormancy period are facilitated.
Preconditions	The valves between the fuel drain tanks and the irradiated fuel containers should be open. The fuel salts are still molten inside the fuel drain tanks.
Systems involved	• Pipes connecting the fuel drain tanks and the irradiated fuel containers • Pipe valves
Interface	Fuel drain tanks and the irradiated fuel containers
Break conditions	Fuel salts transferred to a maximum extent
Postconditions	Molten fuel salts inside the irradiated fuel containers
3. Circulate the Flush Salts and Drain Them to Flush Tanks	
Purpose	To clean up the residual fuel salts inside the reactor core with a flush salt and drain them to the flush tanks
Assumptions	Flush salt is essentially a carrier salt without fissile material. Ready-made flush salts were inside a salt processing cell as a solid state and subsequently heated and melted for this process. They can be directly injected into the reactor core. Flush tanks are located below the reactor core so that the flush salts can be drained by gravity.
Preconditions	Flush salts are molten inside the salt processing cell.
Systems involved	• Salt processing cell • Mechanism to force the circulation (e.g., natural convection, gravity, pump) • Pipes connecting the salt processing cell and the reactor core • Pipe valves
Interface	Salt processing cell and the reactor core
Break conditions	• Circulate the flush salts, maybe multiple times, until the residual fuel salt inside the reactor is wiped out to the maximum extent
Postconditions	The fuel salt inside the reactor has been cleaned up, and the molten flush salt is inside the reactor, waiting to be drained.
4. Transfer the Flush Salts	

Purpose	To transfer the contaminated flush salts from the flush tanks to flush salt containers
Assumptions	The flush tanks are so heavy (in the MSRE case, 4,000kg) that transporting them to the interim storage facility would be unrealistic. By dividing the flush salts into multiple containers that are capable of transport and storage, further processes after the dormancy period are facilitated.
Preconditions	The valves between the flush tanks and the flush salt containers should be open.
Systems involved	• Pipes connecting the flush tanks and flush salt containers • Pipe valves
Interface	Flush tanks and flush salt containers
Break conditions	The flush salts transferred to the maximum extent
Postconditions	Molten flush salts are inside the flush salt containers.
5. Isolate the Salts and Off-Gas System	
Purpose	• To block the migration of hazardous gases to other reactor components • To close any valves connected to the irradiated fuel tanks and the off-gas system
Assumptions	The irradiated fuel tanks and the off-gas system are connected so that the hazardous gases generated from the irradiated fuel salts are captured by the off-gas system.
Preconditions	Irradiated fuel salts are constantly generating hazardous gases, such as volatile fission products, fluorine gas, hydrogen fluoride gas, etc.
Systems involved	• Pipe connecting the irradiated fuel tanks and the off-gas system • Pipe valves • Gas detection equipment placed at other reactor components
Interface	Irradiated fuel tanks and off-gas system vs. other reactor components
Break conditions	No detection of hazardous gases at other reactor components
Postconditions	Irradiated fuel tanks and the off-gas system should be completely isolated, and volatile fission products generated from the irradiated fuel tanks should be captured at the off-gas system, not found at any other places.
6. Dormancy	
Purpose	To reduce the level of heat and radioactivity of the salts, as transporting massive amount of highly radioactive irradiated fuel salts immediately after shutdown is extremely risky
Assumptions	The activity and heat of the irradiated fuel salt precludes or complicates handling and treatment immediately after reactor shutdown.
Preconditions	Fuel and flush salts are isolated inside their respective containers. The off-gas system captures hazardous gases produced from the fuel salts.
Systems involved	• Maintenance systems (e.g., equipment to keep the drain tanks vacuum, ventilation system, off-gas system) • Decay heat cooling mechanism • Gas detection equipment placed at other reactor components
Interface	Maintenance system and the drain tanks
Break conditions	5 years after the fuel discharge
Postconditions	• Decay heat of the irradiated fuel salt is less than 100 W/m^3. • Fuel and flush salts are frozen inside their respective containers.
7. Transfer Irradiated Fuel Containers and Flush Salt Containers to Interim Storage Facility	
Purpose	To transfer the irradiated fuel container and flush salt containers to an interim storage facility *Reason for taking the irradiated fuel and flush salt containers out of the reactor: The drain tank cell should be cleared so that the decontamination and decommissioning of the reactor facility can begin. There are many waste streams other than the salt waste that need to be decontaminated and treated, such as the off-gas stream, operating waste stream, and decontamination and decommissioning waste stream.

Assumptions	• The fuel and flush salts have reached the end of the dormancy period and are able to be transported. • The salt treatment capabilities may not be operational, or the decision to treat has not been made.
Preconditions	The salts are frozen inside the irradiated fuel and flush salt containers.
Systems involved	• Safe and secure transport device • Shielding material for the irradiated fuel containers and the flush salt containers
Interface	Locking mechanism between the irradiated fuel and flush salt containers and the transport device Engineering barriers between the irradiated fuel containers and the flush salt containers cell and the outside air
Break conditions	All irradiated fuel containers and the flush salt containers unloaded to the interim storage facility
Postconditions	Irradiated fuel containers and the flush salt containers are stationed inside the storage facility. Fuel and flush salts are frozen inside the irradiated fuel containers and the flush salt containers.
8. Interim Storage	
Purpose	To store the irradiated fuel and flush salt containers until the treatment capabilities are operational
Assumptions	The salt treatment capabilities may not be operational or decision to treat has not been made. Hence, treating the salts immediately after the dormancy period is impeded, leaving no other option than to temporarily store them. There exists an interim storage facility that accepts irradiated salt containers.
Preconditions	Irradiated fuel and flush salt containers are stationed inside the storage facility. Irradiated fuel and flush salts are frozen inside the containers.
Systems involved	Interim storage facility
Interface	Irradiated fuel and flush salt containers and the storage site beds
Break conditions	All facilities involved in processing the salt wastes available
Postconditions	Both fuel and flush salts are frozen inside the containers and in storage.
9. Transfer Irradiated Fuel and Flush Salt Containers to Respective Treatment Capabilities	
Purpose	• To transfer the irradiated fuel containers to the fuel salt treatment capability • To transfer the flush salt containers to the flush salt treatment capability
Assumptions	All treatment capabilities involved in processing the salt wastes are operational.
Preconditions	Fuel and flush salts are frozen inside the irradiated fuel containers and the flush salt containers.
Systems involved	• Safe and secure transport device • Shielding material for the irradiated fuel containers and the flush salt containers
Interface	Locking mechanism between the irradiated fuel and flush salt containers and the transport device Engineering barriers between the interim storage facility and the outside air
Break conditions	All irradiated fuel containers and the flush salt containers unloaded to the treatment capabilities
Postconditions	Fuel and flush irradiated fuel containers and the flush salt containers are stationed inside the treatment capabilities, and fuel and flush salts are frozen inside the tanks.

3.3.2 Treatment of the Irradiated Fuel Salt Stream

Table 3-4. High-level requirements for the treatment of the irradiated fuel salt stream.

1. Irradiated Fuel Salt: Melting and Redox Control	
Purpose	• To melt the fuel salt to facilitate its chemical control and transfer • To prevent uranium precipitation using redox control, to avoid a criticality safety

	concern
Assumptions	Each irradiated fuel container contains a uranium mass large enough to raise criticality concerns during the melting process, requiring a special redox control procedure.
Preconditions	The irradiated fuel containers and the flush salt containers have been transferred to the fuel salt treatment capability. The fuel salts are frozen inside the irradiated fuel and flush salt containers.
Systems involved	• Heat supply system for melting • Redox control equipment
Interface	Irradiated fuel containers and the heat supply system, irradiated fuel containers and the gas sparging equipment
Break conditions	• Bulk temperature of fuel salts higher than the melting temperature
Postconditions	Fuel salts should be in a molten state without criticality.
2. Irradiated Fuel Salt: Uranium Separation	
Purpose	• To reduce the long-term radionuclide inventory and radioactivity of the fuel salts • To allow for the future reuse of the separated uranium
Assumptions	Uranium separation is permitted by the regulatory bodies. Uranium storage site is available so that the separated uranium can be stored until it is reused.
Preconditions	Fuel salts are molten inside the irradiated fuel container.
Systems involved	• Uranium separation equipment
Interface	Irradiated fuel container and the separation equipment
Break conditions	• Until the uranium is extracted to a maximum extent
Postconditions	Uranium is collected at the separation equipment. Irradiated fuel salt without uranium remains in the irradiated fuel containers in a molten state.
3. Fission Product and Actinide Separation	
Purpose	• To separate the fission products and actinides inside the fuel salt • To reduce the volume of HLW
Assumptions	Fission product and actinides can be separated together to form a single waste stream. Such separation equipment is installed in the fuel salt treatment capability.
Preconditions	Fuel salt without uranium is molten inside the treatment process.
Systems involved	• Fission product and actinide separation equipment
Interface	Separation equipment
Break conditions	• Until the fission product and actinide are extracted to a maximum extent
Postconditions	The fission product and actinide waste stream is deposited inside a separate container, and the carrier fuel salt is left without uranium, fission products, or actinides.

3.3.2.1 *Treatment of the Uranium Stream*

Table 3-5. High-level requirements for the uranium stream.

1. Uranium Conversion	
Purpose	• To convert the collected uranium into a solid uranium tetrafluoride (UF_4) powder • To provide stability for long-term storage and flexibility for reuse
Assumptions	Uranium storage site is available and able to embrace UF_4.
Preconditions	Uranium is collected at the separation equipment. * The form of uranium will depend on which separation was used in the previous step. For example, if a fluorination technique was used, the final form would be UF_6. In that case, a conversion process would not be necessary. On the other hand, if an electrorefining

	techniques was applied, the final form would be uranium metal, where fluorination would be required to produce a UF_4 form.
Systems involved	• Uranium conversion equipment • Equipment to scrape out the extracted uranium
Interface	Equipment holding the extracted uranium and the conversion facility
Break conditions	• Uranium converted into UF_4 to a maximum extent
Postconditions	Uranium is in a UF_4 form and ready for packaging. Raffinate salts are being handled simultaneously.
2. Uranium Containerization	
Purpose	• To put the converted UF_4 powder into storage containers • To weld the containers to prevent any leakage of uranium
Assumptions	Uranium storage site is available and able to embrace UF_4. The UF_4 storage container has been designed to meet the technical criteria, including the corrosion issues.
Preconditions	Uranium has been separated to a targeted amount. The converted UF_4 powder meets the waste acceptance criteria.
Systems involved	• UF_4 storage container • Welding equipment • Device to transfer the UF_4 powder into the containers
Interface	Uranium conversion equipment and the transfer device, transfer device and the storage containers
Break conditions	• Containers meeting the waste acceptance criteria of the storage site • Welded containers
Postconditions	UF_4 container is ready for transport.
3. Uranium Transport	
Purpose	• To transport the UF_4 containers to a storage site
Assumptions	Uranium storage site is available. The transport device and processes meet the transportation criteria.
Preconditions	The solid UF_4 powder is containerized.
Systems involved	• Safe and secure transport device • Security force • UF_4 storage facility
Interface	Locking mechanism between the UF_4 container and the transport device
Break conditions	• All UF_4 containers unloaded to the storage site
Postconditions	UF_4 containers are unloaded at the storage site.
4. Uranium Storage	
Purpose	• To dock the UF_4 containers to the storage site beds • To store the uranium resources until they are to be reused
Assumptions	Uranium storage site is available.
Preconditions	UF_4 containers are unloaded at the storage site.
Systems involved	• Uranium storage facility
Interface	UF_4 containers and the storage site beds
Postconditions	UF_4 is stored at the storage site, waiting for future reuse.

3.3.2.2 *Treatment of the Fission Product and Actinide Stream*

Table 3-6. High-level requirements for the fission product and actinide waste stream.

1. Fission Product and Actinide: Waste Form Development	
Purpose	• To immobilize the fission products and actinides into a waste form that could be accepted at HLW disposal facility
Assumptions	The separated fission product and actinide waste stream is classified as HLW. The immobilization technique can simultaneously hold both fission products and actinides stably so that they do not diffuse outside of the waste package.
Preconditions	Fission product and actinide waste streams are deposited inside separate containers.
Systems involved	• Containers holding the fission product and actinide waste stream • Equipment for developing waste forms
Interface	Equipment for developing waste forms and the waste stream
Break conditions	• Produced waste form meets site criteria
Postconditions	Fission products and actinides are immobilized into a waste form, and they are still inside the initial separate containers.
2. Fission Product and Actinide: Containerization	
Purpose	• To pour the immobilized wastes into encapsulation containers • To weld the encapsulation containers to prevent any leakage of radionuclide
Assumptions	An operating disposal facility that accepts immobilized HLW exists. The encapsulation container has been designed to meet the site criteria.
Preconditions	The immobilized fission product and actinide waste stream is inside a separate container.
Systems involved	• Encapsulation container • Welding equipment • Equipment to pour the immobilized waste into the encapsulation container
Interface	Between the pouring equipment and the encapsulation container and a locking mechanism between the container and its lid
Break conditions	• Containers meeting the waste acceptance criteria of the disposal facility
Postconditions	Immobilized waste is solidified inside the encapsulation container. The encapsulation containers are completely sealed and ready for transport.
3. Fission Product and Actinide: Transport	
Purpose	• To transport the encapsulation container to a disposal facility
Assumptions	An operating disposal facility that accepts immobilized HLW exists. The wastes meet the waste acceptance criteria of the disposal facility.
Preconditions	Immobilized fission product and actinide waste are solidified inside the encapsulation containers, packaged for transport
Systems involved	• Safe and secure transport device • Security force
Interface	Locking mechanism between the container and the transport device
Break conditions	• Until all containers are unloaded to the disposal facility
Postconditions	The containers are stationed inside the disposal facility.
4. Fission Product and Actinide: HLW Disposal	
Purpose	• To dock the fission product and actinide waste containers to the disposal site beds • To dispose of the highly radioactive fission product and actinides where it would be safe for millions of years

Assumptions	An operating disposal facility that accepts immobilized HLW exists.
Preconditions	The encapsulation containers have been stationed inside the disposal site.
Systems involved	• HLW disposal facility
Interface	FP and Ac containers and the HLW disposal site beds
Postconditions	FP and Ac are permanently disposed of at the HLW disposal facility.

3.3.2.3 *Treatment of the Carrier Salt Stream*

Table 3-7. High-level requirements for the carrier salt stream.

1. Carrier Salt: Treatment	
Purpose	• To treat the carrier salt into a form that meets the acceptance criteria of the storage facility (e.g., ensuring a solid waste form, compaction, immobilization)
Assumptions	The carrier salt refers to an irradiated fuel salt whose uranium, actinides, and fission products have been removed. This carrier salt requires no further separation of radionuclides to be treated and transported.
Preconditions	The carrier salt is molten inside some tanks after fission product and actinide separation.
Systems involved	• Treatment equipment
Interface	Treatment equipment and the carrier salt
Break conditions	• Approved treated carrier salt • Sealed salt storage container is sealed
Postconditions	The carrier salt is in a solid state, isolated inside the storage container.
2. Carrier Salt: Containerization	
Purpose	• To transfer the treated carrier salt from the tanks to salt disposal containers
Assumptions	The carrier salt treatment is complete. The radionuclide content will be very small, compared to fuel salts.
Preconditions	Carrier salts are molten inside tanks. Salt storage containers and tanks are connected via a transfer system.
Systems involved	• Salt storage containers • Salt transfer system
Interface	Salt storage containers and the tank containing the carrier salt
Break conditions	• The carrier salt transferred to the storage containers to a maximum extent
Postconditions	Carrier salts are contained inside the storage containers.
3. Carrier Salt: Transport	
Purpose	• To transport the carrier salt containers to a storage facility
Assumptions	A facility to store the treated carrier salts exists.
Preconditions	Carrier salts are chemically and radiolytically stable. Containers are sealed and packaged for transport.
Systems involved	• Safe and secure transport device
Interface	Locking mechanism between the transport device and the container
Break conditions	• Until all containers are unloaded to the storage facility
Postconditions	The containers are stationed inside the storage facility.
4. Carrier Salt: Disposal or Reuse	

The final option for the carrier salt will not be explicitly determined in this study.

3.3.3 Flush Salt Stream

Table 3-8. High-level requirements for the flush salt stream.

1. Flush Salt: Melting	
Purpose	• To melt the flush salts to facilitate chemical control and salt transfer
Assumptions	The flush salts contain only a little amount of uranium, thus no redox control is required during the melting process.
Preconditions	The flush-salt containers have been transferred to the flush salt treatment capability. The flush salts are frozen inside the flush salt containers.
Systems involved	• Heat supply system for melting
Interface	Flush salt containers and the heat supply system
Break conditions	• Bulk temperature of fuel salts higher than the melting temperature
Postconditions	Flush salts should be molten inside the flush salt treatment capability.
2. Flush Salt: Treatment	
Purpose	• To treat the flush salts into a form that meets the acceptance criteria of the storage facility (e.g., ensuring a solid waste form, compaction, immobilization)
Assumptions	The flush salt is classified as LLW. An operating LLW storage facility that accepts salt wastes exists.
Preconditions	The flush salt is molten inside the flush salt treatment container.
Systems involved	• Treatment equipment
Interface	Treatment equipment and the flush salt
Break conditions	• Treated flush salt meeting the site criteria
Postconditions	The treated flush salt is ready to be packaged.
3. Flush Salt: Containerization	
Purpose	• To transfer the treated flush salt from the flush salt treatment equipment to storage containers
Assumptions	The flush salt treatment is complete. The radionuclide content will be very small, compared to fuel salts.
Preconditions	Molten flush salts are inside the flush- salt treatment equipment. Salt storage containers and the flush salt treatment equipment are connected via a transfer system.
Systems involved	• Salt storage containers • Salt transfer system • Flush salt treatment equipment
Interface	Salt storage containers and the flush salt treatment tank
Break conditions	• Flush salt transferred to the storage containers at a maximum extent
Postconditions	Flush salts are contained inside the storage containers.
4. Flush Salt: Transport	
Purpose	• To transport the flush salt containers to a storage facility
Assumptions	Salt storage facility for salts should be available. The treated flush salts and its container meets the acceptance criteria of the storage facility.

Preconditions	Flush salts are chemically and radiolytically stable. Containers are sealed and packaged for transport.
Systems involved	• Safe and secure transport device
Interface	Locking mechanism between the transport device and container
Break conditions	• Until all containers are unloaded to the storage facility
Postconditions	The containers are stationed inside the storage facility.
5. Flush Salt: Disposal or Reuse	
The final option for the flush salt will not be explicitly determined in this study.	

4. CRITICALITY ANALYSIS

This section describes an analysis of the criticality safety of a proposed salt container system to determine the number of containers needed to hold the irradiated fuel salt during the dormancy and interim storage period under a number of scenarios. The analysis assumes that the most conservative scenario was a system where all the irradiated fuel salt is put into a single container and taken as the nominal condition and then postulates some credible off-nominal conditions. Based on those conditions, the criticality safety of the storage system is evaluated by calculating the effective neutron multiplication factor (k_{eff}) for various scenarios using the MCNP radiation transport code. The fuel salt was modeled using MSRE fuel salt characteristics, including fuel salt composition, uranium enrichment, fuel salt density, and volume.

4.1 Methodology

To judge the criticality safety of the proposed irradiated fuel salt storage systems, a criticality safety limit should be established. Per the guidance in ANSI/ANS-8.24, *Validation of Neutron Transport Methods for Nuclear Criticality Safety Calculations*[8], this limit should be based on the bias and bias uncertainty of MCNP for similar critical benchmarks, as shown in Eq. (4.1).

Here, is the upper subcritical limit, above which the system cannot be proven to be subcritical. represents the calculation margin, a combination of the bias and bias uncertainty, and represents the margin of subcriticality. Only cases that meet the condition presented in Eq. (4.2) can be proven to be subcritical.

In this report, the baseline USL is determined using MCNP's Whisper software. Whisper was run using six distinctive cases from the various scenarios presented in this section, organized in Table 4-1. These cases are disparate from each other in terms of the number of containers, lattice type of the containers' configuration, weight fraction of water ingress, height-to-diameter ratio of each container, and spacing between the containers. Such heterogeneousness should provide a wide range of neutronic profiles to test the applicability for the benchmark cases present in the Whisper suite.

The baseline USL values were calculated for each case to find the lowest value, which turned out to be 0.95270 for Case 6. An additional margin of 0.01 was subtracted from the lowest USL due to the low correlation coefficients for the most similar benchmark experiments. This is recommended by the MCNP team for any case where the highest $C_k < 0.8$.[9] The margin was conservative since Whisper did not calculate a noncoverage penalty for these input files. Hence, the USL used in the criticality analysis of this study is 0.94270.

Table 4-9. Summary of cases used to search for the upper subcritical limit.

Case #	Number of Containers	Lattice Type	Water Weight Fraction (%)	H/D Ratio of Each Container	Spacing Between Containers (cm)	USL
1	1	Square	0	1	N/A	0.95386
2	36	Square	10	1	50	0.95714
3	36	Square	10	1	0.0001	0.96920
4	36	Hexagonal	0.1	1	0.0001	0.96898
5	36	Hexagonal	10	5	7	0.97183
6	100	Square	10	1	50	0.95270
Upper subcritical limit for this study						0.94270

4.2 Nominal Conditions

4.2.1 Single Container System

Description of the Input

The system geometry is illustrated in Figure 4-1. Although spherical shapes are frequently employed in criticality searches, a salt container is unlikely to be in such a shape. Rather realistically, the model assumed that the salt container will be cylindrical. An infinite water reflection was modeled around the system for conservativism. Using convention, the water reflector thickness was set as 12 in. The fuel salt is contained in a cylindrical tank, surrounded by 12 in. of water reflector. The fuel salt density at 911 K is 2.3275 g/cm^3.[10] The density of the water was simply set as 1 g/cm^3.

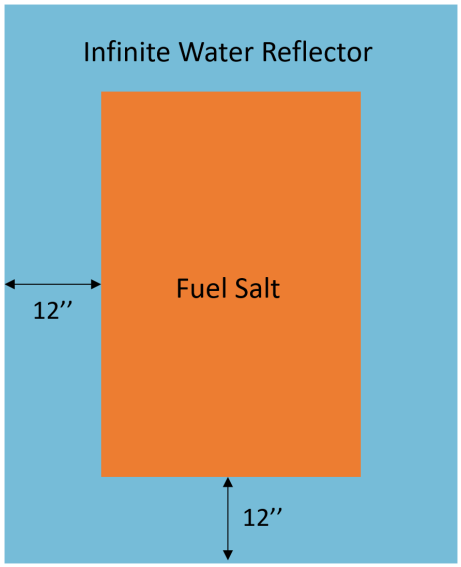

Figure 4-5. Frontal cross section of the salt container.

To check the geometry effect on criticality, the height-to-diameter ratio of the system was varied and the effective multiplication factor calculated. Three values were used as the height-to-diameter (H/D) ratio of the fuel salt tank: 0.5, 1.0, and 2.0.

A key variable was the mass of U-235 inside the fuel salt. As MSRE was initially loaded with 200–250 kg of uranium, and approximately 31 wt% of it was U-235. The mass of U-235 ranged from 65 to 75 kg. Based on the mass of U-235 and the H/D ratio, the mass, volume, and geometry of the fuel salt tank were estimated. The tank is filled with 100% fuel salt.

The fuel salt composition was also based on MSRE data. The initial fuel salt was LiF-BeF_2-ZrF_4-UF_4 (65 mol%-29 mol%-5 mol%-1 mol%), with some impurities. Some elements, such as Cr, Fe, Ni, and Hf, dissolved out from the structural material into the salt during the initial operation. The composition of a fresh fuel salt, not an irradiated fuel salt, was used as the input to produce as conservative a k-value as possible. Also, the abundances of all isotopes except for Li and U were assumed to be following the natural abundances.[11] In MSRE, Li-7 was enriched to 99.995 wt% to prevent tritium production, and U-235 was enriched to about 31 wt%. Table 4-2 shows the weight fractions of each isotope inside the fuel salt. It was assumed that all these isotopes are homogeneously mixed inside the container.

Table 4-10. Abundance and weight fractions of nuclides comprising the fresh fuel salt.[10]

	Nuclide	**Abundance**	**Weight Fraction**
Li	Li-6	0.00005	4.6967E-06
	Li-7	0.99995	1.0956E-01

Be	Be-9	1	6.3491E-02
O	O-16	0.99757	4.8865E-04
	O-17	0.00038	1.9784E-07
	O-18	0.00205	1.1301E-06
F	F-19	1	6.7026E-01
Cr	Cr-50	0.04345	1.1687E-06
	Cr-52	0.83789	2.3436E-05
	Cr-53	0.09501	2.7086E-06
	Cr-54	0.02365	6.8694E-07
Fe	Fe-54	0.0585	9.1454E-06
	Fe-56	0.9175	1.4887E-04
	Fe-57	0.0212	3.4997E-06
	Fe-58	0.00282	4.7390E-07
Ni	Ni-58	0.68077	2.0161E-05
	Ni-60	0.26223	8.0332E-06
	Ni-61	0.011399	3.5503E-07
	Ni-62	0.036346	1.1505E-06
	Ni-64	0.009255	3.0243E-07
Zr	Zr-90	0.5145	5.6288E-02
	Zr-91	0.1122	1.2412E-02
	Zr-92	0.1715	1.9180E-02
	Zr-94	0.1738	1.9861E-02
	Zr-96	0.028	3.2678E-03
Hf	Hf-174	0.0016	8.6548E-09
	Hf-176	0.0526	2.8780E-07
	Hf-177	0.186	1.0235E-06
	Hf-178	0.2728	1.5096E-06
	Hf-179	0.1362	7.5794E-07
	Hf-180	0.3508	1.9631E-06
U	U-234	0.3163	1.4375E-04
	U-235	0.0032	1.4094E-02
	U-236	0.0013	5.9265E-05
	U-238	0.6792	3.0653E-02

Results

The k_{eff} value for varying U-235 masses and varying H/D ratio were calculated using MCNP with an associated standard deviation. The results are plotted in Figure 4-2. The most important observation from this simulation result is that the largest k_{eff} value was 0.87303, which is under the assumed criticality safety value of 0.94270. This implies that, even when all the fuel salts are poured into a single tank, the system will be subcritical. It is worth noting that the calculation approach was very conservative, such as the fuel composition being equal to that of a fresh fuel, a reflection provided by an infinite water reflector, an absence of neutron absorbers, etc., providing an extra margin for criticality.

The overall trend was that the increase in U-235 caused an increase in k_{eff}. This trend is obvious, as the increase in fissile material enables more fissions to occur, leading to an increase in the k_{eff} value. Although some data points seem to deviate from this increasing trend, if the standard deviations arising from the Montel Carlo simulation are considered (refer to the error bars in Figure 4-2), these data points

do not harm the increasing trend.

The effect of geometry on criticality could be found, too. A larger H/D ratio allows for the storage of more mass in a single cylinder due to higher surface-to-volume ratios, which promotes neutron leakage. This effect is shown by the difference among the k_{eff} values of H/D = 0.5, 1.0, and 2.0. The geometries with an H/D of 1.0 had the largest k_{eff} values, followed by an H/D of 0.5 and then 2.0.

Figure 4-6. Effect of varying U-235 mass on the criticality in a single container system.

4.3 Off-Nominal Conditions

Prior to setting up an off-nominal situation for the salt container, several scenarios that might affect the criticality were investigated. For that, the main parameters that influence the criticality of a system were reviewed, namely mass, absorption, geometry, interaction, concentration, moderation, enrichment, reflection, and volume (as known as MAGIC MERV). Some possible abnormal situations that affect each parameter were identified. The following table organizes the logic behind the postulated scenarios and whether the scenario will be quantitatively evaluated or not.

Table 4-11. Investigation on the possible abnormal situations that influence MAGIC MERV.

Parameters	Possible Abnormal Situations	Will It Be Quantitatively Evaluated?
Mass	During the transfer of salts from the drain tanks into the container, the salts can spill or leak to the floor out of the pipes. In that case, the mass of the salt can change, but it would not be a concern as the reactivity will decrease.	X
Absorption	Absorption was not credited in these analyses. The presence of neutron-absorbing materials in the container provides an undefined, real benefit to the system.	X
Geometry	The salts will be transferred from the drain tanks into the containers through the pipes, not by pouring the salts. In that case, the geometry of the salts will not significantly differ from the original cylindrical form.	X
Interaction	If the number of containers is more than one, the spacing between the containers comes into play. Criticality might be achieved when the containers are accidently placed close to each other, even if the individual containers were at a subcritical condition.	O
Concentration	The concentration of uranium and other nuclides cannot be changed once the fuel salt is withdrawn from the reactor. The fuel composition depends on the operational history.	X
Moderation	The bounding, credible abnormal scenario is the increase in moderation due to an accidental ingress of water. This could occur during the transfer of fuel salts from the drain tank into the containers.	O
Enrichment	No scenarios that could change the enrichment of U-235 in the fuel salt have been identified.	X
Reflection	According to Figure 4-1, an already infinite reflection is being provided by water. No further abnormal scenarios can change this parameter.	X
Volume	No scenarios that could change the volume of the salt containers have been identified. The volume of each salt container depends on the total volume of salt and the number of containers.	X

The accident scenarios that were considered credible and could affect the criticality of the system were determined to be water ingress into the salt container and the change in spacing between containers. As the latter scenario assumes that the number of containers is more than one, this scenario was not

evaluated for the single container system (Section 4.3.1). For the multiple container system (Section 4.3.2), both scenarios were investigated.

4.3.1 Single Container System

Description of the Input

Suppose a situation where molten fuel salts are transferred from the drain tanks to the containers through the pipes and water accidently breaks into the containers. The water content will enhance the neutron moderation, causing an increase in reactivity (assuming that the MSR was a thermal reactor). Although it has been confirmed in Section 4.3.1 that a single container is sufficient to store the fuel salts without causing criticality, this might not be the case when water breaks in. Thus, a scenario where water breaks into a single container holding of the entirety of the fuel salt was evaluated.

In this scenario, the weight fraction of water ingress was varied from 0.1 to 10 wt%. The geometry of the container still follows the configuration shown in Figure 4-1: a cylindrical salt container surrounded by a 12-in.-thick water reflector. Since it has been confirmed from Section 4.2.1 that a cylinder where H/D = 1.0 produces the most conservative effective k-value, this geometry will be adopted in this calculation.

The composition of each isotope inside the fuel salt was again assumed to be following the values in Table 4-2. The mass of the water was calculated using Eq. (4.3), where the mass of the salt is deduced from the initial mass of U-235 and its weight fraction. Here, the mass of U-235 was assumed to be 68 kg, referring to the initial loading of U-235 at the beginning of the MSRE operation.

Note that water is assumed to be mixed homogeneously with the fuel salt. This assumption is not realistic, as the density difference between the water and salt will cause the water to float above the salt. However, this assumption leads to a more conservative k_{eff} value.

Results

The simulation results are plotted in Figure 4-3, describing the effect of the weight fraction of water ingress on the k_{eff} value. An increasing trend in k_{eff} was observed as the weight fraction of water increased. This is because moderation is enhanced as the weight fraction of water increases. The single container k_{eff} was 0.88 without water ingress, and exceeded the USL when the water ingress was only 0.4 wt%. From these results, a single container cannot store all of the fuel salts safely during abnormal conditions. Thus, the salts must be divided into multiple tanks to maintain criticality safety.

Figure 4-7. Effect of water ingress on criticality in a single container system.

4.3.2 Multiple Container System

4.3.2.1 *Square Lattice*

Description of the Input

From the results in Section 4.2.1, the fuel salts must be stored in multiple containers in case of water ingress to maintain criticality safety. To decide the minimum number of tanks required for safety, the number of containers was increased one by one until the system is subcritical under a substantial amount of water ingress.

The geometry of the individual container will still follow the configuration seen in Figure 4-4. In addition, the distance between the containers affects the interaction parameter of MAGIC MERV and so is varied as a parameter of investigation. Note that the "distance between the containers (*d*)" refers to the edge-to-edge distances, not the center-to-center distances. Thus, the minimum spacing between the containers was determined by varying the distance between containers, from 10 to 200 cm in increments of 10 cm when considering two-container and three-container systems. For systems with four or more

containers, the distance was investigated at 0.0001, 10, 25, and 50 cm.

Figure 4-4 illustrates the cross-sectional view of the multiple container systems. The center circle (orange) refers to the fuel salt and the outer annulus (blue) refers to the 12-in. water reflector. The two-container system is simply aligned in a straight line, and the three-container system is in a regular triangle. For four-, nine-, 16-, 25-, 36-, 49-, 64-, 81-, and 100-container systems, they are shaped in a square of 2 × 2, 3 × 3, 4 × 4, 5 × 5, 6 × 6, 7 × 7, 8 × 8, 9 × 9, and 10 × 10 arrays, respectively.

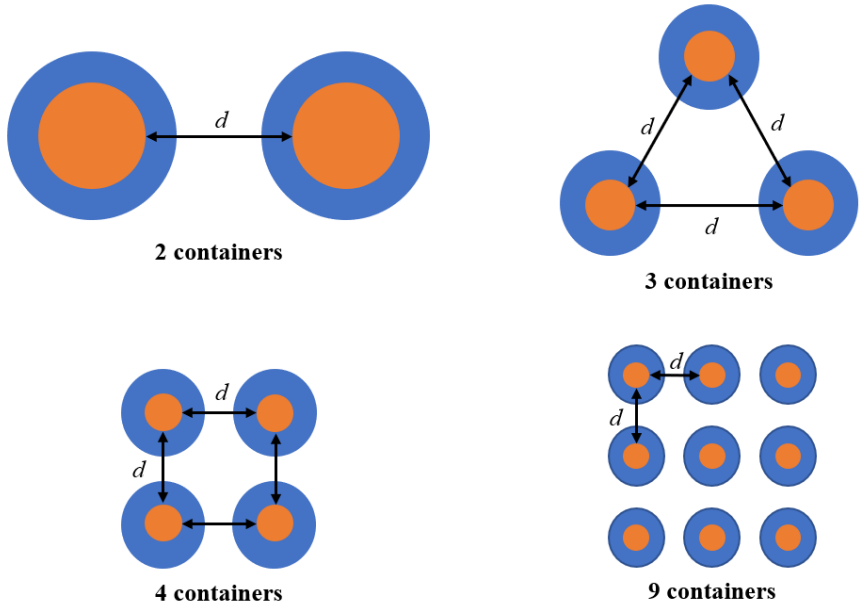

Figure 4-8. Cross-sectional view of the configuration of two, three, four, and nine containers (orange=fuel salt, blue=water reflector, d=distance between the containers).

Results

The effective k-values for various numbers of containers are plotted in Figure 4-5 and Figure 4-6. The most notable finding was that, even if the salt is divided into 100 containers, if the containers are in contact with each other () with a significant water ingress (10 wt%), the system was still exceeding the USL. This result shows that some configuration control may be needed for criticality safety to be maintained. For configurations with a distance between containers of 10 cm or larger, the k_{eff} value began to drop below the USL even under the maximum water ingress when the number of containers was equal to or more than 36. Thus, the minimum number of fuel salt containers is 36, and the distances between the containers should be at least 10 cm. Depending on the container and storage system design, an engineering feature such as a spacer grid may be needed. Or alternatively, the H/D ratios of the containers can be increased to provide a favorable geometry for criticality safety, thus enabling a denser packing of containers without any spacer grids. These options will be investigated later in Section 4.3.2.2.

Figure 4-9. Effect of water ingress on criticality in a square lattice system for various spacings in two-, three-, four-, 9-, 16- and 25-container systems (the legends denote the spacings in cm).

Figure 4-10. Effect of water ingress on criticality in a square lattice system for various spacings in 36-, 49-, 64-, 81-, and 100-container systems (the legends denote the spacings in cm).

4.3.2.2 *Hexagonal Lattice*

Description of the Input

So far, the containers were assumed to be arranged in a square lattice. However, the containers can be stored in a more volume-efficient manner using a hexagonal lattice. Thus, this section examines the changes in criticality safety when the containers are reconfigured to a hexagonal lattice.

The conditions assumed in this section are similar to those in Section 4.3.1: same thickness of water reflector, same fuel salt composition, H/D ratio constant as 1, and the range of weight fraction of water ingress. The differences are that the number of containers will be fixed at 36, the lattice will be hexagonal, and the candidates for the distance between containers will be 6, 7, 8, and 9 cm. The number 36 has been chosen from the conclusions in Section 4.3.2.1. The hexagonal lattice configuration is depicted in Figure 4-7. The pink circles represent the cross-sectional views on the fuel salts, and the blue space depicts the water reflectors surrounding each fuel salt container.

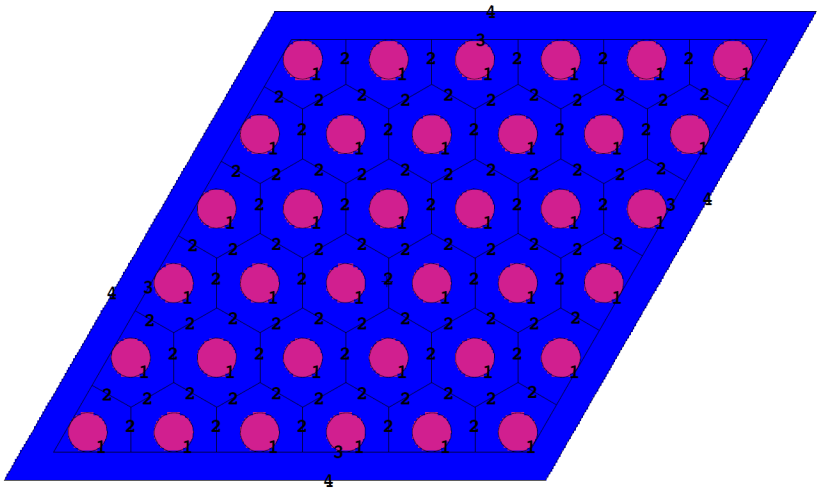

Figure 4-11. Cross-sectional view of a storage system arranged in a hexagonal lattice.

Results

Using the input parameters described above, MCNP calculated the effect of water ingress on criticality for various spacing between the containers. The k_{eff} values as a function of the weight fraction of water are plotted in Figure 4-8. The results clearly show that the system is subcritical at all spacings. The k_{eff} reached the maximum value of 0.92585 at 10 wt% for a 6 cm spacing, which is still under the USL. To check the advantage of transforming the container configuration from a square lattice into a hexagonal lattice, the system volumes were compared between the two lattice types for each spacings (see Figure 4-9). Here, the system volume refers to the volume inside the boundaries of the outermost water reflectors. It turned out that the system volumes of hexagonal lattice systems were always smaller than those of square lattice systems, for all spacings. In sum, by reconfiguring the lattice type into a hexagonal

lattice, the containers may be stored in a more compact manner while satisfying criticality safety.

Figure 4-12. Effect of water ingress on criticality in a hexagonal lattice system with 36 containers, for spacings of 6, 7, 8, and 9 cm.

Figure 4-13. System volume of square and hexagonal lattice system with 36 containers, for spacings of 6, 7, 8, and 9 cm.

In reality, it is difficult to maintain a distance larger than 2 cm between the storage containers and thus a mechanical spacer should be used. Or alternately, a passive safety feature can be added by simply making the containers thinner and taller. If the thin and tall containers can provide enough of a criticality safety margin, it is possible that the containers can be packed more densely so that a mechanical spacer is not required. This possibility is discussed next.

4.3.2.3 *Hexagonal Lattice with Larger H/D Ratios*

Description of the Input

From the results in Section 4.3.2.2, the system is subcritical for 0.1–10 wt% of water ingress at spacings of 6, 7, 8, and 9 cm. This implies that it is necessary to either use engineered safety feature equipment to keep the containers apart or use a passive safety feature like increasing the H/D ratio of the containers to maintain criticality safety. Since increasing the H/D ratio of the containers is one of the most favorable options to provide a passive safety feature, this section will be devoted to investigating the k_{eff} values when the H/D ratios are increased to 2, 3, 4 and 5 under maximum water ingress situation. At the same time, the spacing between the containers will be varied from 0.0001 to 9 cm. Other conditions, such as the lattice type (Figure 4-7), fuel salt composition (Table 4-2), number of containers, and the thickness of water reflector, remain the same.

Results

Using the input parameters described above, the k_{eff} values were calculated via MCNP. Figure 4-10 is a plot of k_{eff} values as a function of the spacing between containers for various H/D ratios. There are two main observations from this plot:

(a) The k_{eff} value decreased as the spacing between the containers increased. When the containers were almost in contact with each other (0.0001 cm), the k_{eff} value increased as the H/D ratio increased. This is an unexpected trend, as the k_{eff} value of a thin, tall container was expected to be lower than that of a wide, short cylinder. But this trend was reversed when the spacing increased to over 6 cm: the k_{eff} value decreased as the H/D ratio increased.

(b) Additionally, the change in k_{eff} values due to the increase in spacing was more noticeable for containers with large H/D ratios. For example, the k_{eff} value decreased from approximately 1.4 to 0.8 for H/D=5, while the value decreased from almost 1.2 to 0.9 for H/D=1.

Figure 4-14. Effect of spacing between containers on criticality in a hexagonal lattice system with 36 containers, for various H/D ratios.

These observations can be understood by looking at the container system as a whole, not at the individual containers. When the spacing between containers is very small, the containers are almost arranged in clusters, and thus the system can be approximated as a lump of fuel salt. In a hexagonal lattice system like this, such a lump can be described as a parallelepiped whose height (H) is identical to that of the individual containers and width (W) is the sum of the diameters of six containers plus the spacing between them (see Figure 4-11). To quantitatively understand the geometry of this parallelepiped, the

system height-to-width (H/W) ratios were calculated for each spacing and H/D ratio, as shown in Figure 4-12.

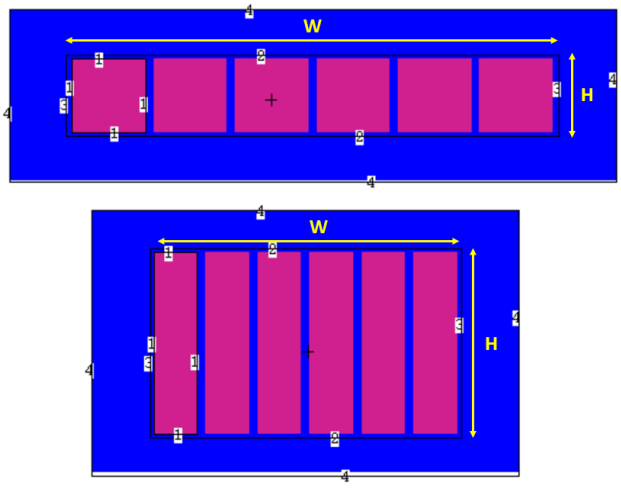

Figure 4-15. Frontal cross sections of hexagonal lattice systems with 36 containers, with H/D=1 (top) and 5 (bottom).

Figure 4-16. System H/W ratio in a hexagonal lattice system with 36 containers, with various spacings and H/D ratios.

The system H/W ratios are closer to unity as the H/D ratio is increased. Comparing them with the k_{eff} values in Figure 4-10, the k_{eff} values were high when the H/W ratio was close to unity, resembling the behavior of a single container. For instance, the maximum H/W is 0.833 when the spacing is 0.0001 cm and the H/D is 5, the very case where the system reaches the maximum k_{eff} value of 1.403. From this observation, the unusual trend found in (a) might be better understood. Also, the reverse in this trend of spacings larger than 6 cm can be explained by considering that the system deviates from a simple lump of fuel salts as the spacing between the containers becomes nonnegligible. As the spacing increases, the interactions between containers weaken, letting the H/D ratio effect dominate, and thus the expected criticality trend comes into view.

The trend described in (b) can be interpreted in a similar manner. A container with H/D=1 has a radius of about 22 cm, and a container with H/D=5 has a radius of about 13 cm. As the spacing between the containers is increased by 1 cm, the “1 cm” is observed differently for those two cases: the latter will be more sensitive to the 1-cm change than the former. This is quantitatively proved in Figure 4-12: for large H/D container systems, the H/W ratios decrease more steeply as the spacings increase, thus the k_{eff} values also decrease more steeply. In this way, the sensitivity of k_{eff} values for large H/D container systems can be construed.

This section concludes that increasing the H/D ratio of a container does not necessarily guarantee criticality safety under water ingress scenarios. Doing so may make the system more sensitive to the spacing between the containers. In our configuration, it proved that securing a certain amount of spacing becomes more crucial, especially for a thin and tall container system. These results recommend that the containers be spaced sparsely with the assistance of an engineering spacer, rather than merely increasing the H/D ratio and keeping the spacings dense. For example, referring to the operational requirements of commercial spent fuel storage system that require the k_{eff} value to be maintained under the U.S. Nuclear Regulatory Commission criticality limit of 0.95, the H/D ratio must be larger than 3 and the spacing should be larger than 7 cm.

5. DECAY HEAT AND DOSE RATE ANALYSIS

Section 3 proposed that a certain length of dormancy is required before the irradiated fuel salt management process starts. This would allow the irradiated fuel salt to decay below a threshold activity and decay heat level under which they can be handled and treated. To determine the length of this dormancy period, the radioactivity and decay heat of the irradiated fuel salt as a function of time must be understood. In this section, the decay heat of the irradiated fuel salt is calculated with the aid of ORIGEN module in the SCALE suite of codes, and the results are utilized to calculate the neutron and gamma dose inside the storage system, again using MCNP.

5.1 Decay Heat Analysis

Description of the Input

In Section 0, the criticality safety of the storage containers was analyzed based on the fresh fuel composition of MSRE for conservatism. However, for the radioactivity and decay heat of the fuel salts, the irradiated fuel composition must be used, since this will produce the most conservative results. Thus, the composition of the irradiated fuel salt was assumed based on the end-of-life composition of MSRE, organized in Table 5-1.[12]

Note that there are some isotopes that could not be included in this analysis due to lack of data: Pd, Rb, Mo, I, La, Nd, Gd, Pb, Po-213, At-217, Fr-221, Ra-225, Ac-225, Th-229, U-235, U-236, and U-238. For these species, they were assumed to be not included in the irradiated fuel salt. This omission could lead to some uncertainties in the decay heat calculations in the short term. However, since the time scale of the dormancy or storage period is much longer than most of the half-lives of these species, these uncertainties will make only marginal errors in deciding the dormancy period.

While most of these missing fission products and lanthanides are not expected to cause noticeable errors in the long term, the absence of iodine (I) could be the biggest source of error in the long-lived gamma activity. I-129 is known as a long-lived fission product whose half-life is about 15.7 million years, emitting beta and gamma. But as the decay heat and energy from this isotope (194 keV) is relatively low compared to those of Cs-137 and Sr-90, the calculation will be conducted without the radioactivity information of I-129.

Also, the U species consisted of U-233 instead of U-235. While MSRE was initially fueled with U-235, ORNL later refueled the reactor with U-233 during its operations. Thus, the end-of-life composition does not exactly match with the fresh fuel data. However, both U-233 and U-235 decay very slowly and do not noticeably contribute to the radioactivity and decay heat inside an irradiated fuel. Thus, the difference in the uranium species is not expected to cause a substantial uncertainty.

Table 5-12. Irradiated fuel salt composition and the radioactivity of each isotope at discharge.[12]

Element	Z	A	Radioactivity [Ci]	Element	Z	A	Radioactivity [Ci]
Fission Products				Ac-Decay Daughters			
Sr	38	89	1.62E+05	Pm	61	147	3.72E+04
		90	1.40E+04			148	0.00E+00
Y	39	90	1.36E+04			148m	1.05E+03
		91	1.83E+05	Sm	62	151	1.47E+02
Zr	40	93	3.00E-01	Eu	63	152	5.50E+00
		95	2.00E+05			154	3.52E+01
Nb	41	95	1.73E+05			155	3.76E+02
		95m	4.15E+03	Transuranic Elements			
Tc	43	99	5.00E-01	Tl	81	208	5.48E+01
Ru	44	103	7.40E+04			212	1.53E+02
		106	7.42E+03	Bi	83	212	1.52E+02
Rh	45	103m	7.39E+04	Po	84	212	9.75E+01
		106	8.93E+03			216	1.53E+02
Sb	51	125	6.47E+02	Rn	86	220	1.53E+02
Te	52	125	1.87E+02	Ra	88	224	1.53E+02
		127	3.27E+04	Th	90	228	1.53E+02
		127m	3.94E+03	U	92	232	1.73E+02
		129	9.78E+04			233	3.02E+02
		129m	2.67E+04			234	1.74E+01
Cs	55	134	5.50E+00	Pu	94	238	1.00E+00
		137	1.12E+04			239	4.17E+01
Ba	56	137m	1.05E+04			240	1.53E+01
Ce	58	141	4.10E+05			241	9.04E+02
		144	1.27E+05	Am	95	241	9.60E-01
Pr	59	144	1.28E+05	Cm	96	242	2.45E+01

Based on the composition assumed above, the decay heat generated from each isotope was calculated as a function of time after discharge, specifically at 0, 1, 7, 14, 30, 60, 90, 180, 365, 730, 1825, and 3650 days after discharge. It is assumed that the fuel salts are drained into drain tanks right after reactor shutdown and subsequently transferred to 36 irradiated fuel containers. Thus, the decay heat produced from the total fuel salt is divided by 36 for each tank.

Results

Using the ORIGEN module, the decay heat produced from a unit volume of irradiated fuel salt was calculated. According to Figure 5-1, 1 m^3 of irradiated fuel salt produces about 2,564 W of heat immediately after discharge. Until the decay heat drops below 2,000 W/m^3, which is expected to be at least 30 days after discharge, the fuel salt drain tanks should be supplied with an active cooling system. In 90 days, the decay heat reduces by half. And after 5 years, it declines to 96.82 W/m^3. From this point, the decay heat should not challenge moving on to the next irradiated fuel management step: transferring the fuel salt from the drain tanks into 36 storage containers.

Figure 5-17. Decay heat from a single drain tank as a function of time after discharge.

The amount of decay heat here is relatively low compared to that of commercial nuclear power plants because of the differences in thermal outputs: 8 MWt at MSRE vs. 3,000 MWt at pressurized-water reactors. As the thermal output of the experimental MSR that will be built at the LOTUS test bed is expected to be smaller than 500 kWt, the decay heat from this reactor should be lower than that described here. Thus, the dormancy period proposed based on the MSRE data will be sufficient for the LOTUS test bed but not applicable for future commercial MSRs.

The ORIGEN module was also used to calculate the contribution to decay heat production for each isotope, as shown in Figure 5-2. As expected, the Cs-137 and Sr-90 groups started to take up large portions of decay heat from 5 years after discharge. Y-90, the decay product of Sr-90, produces 2.28 MeV of decay energy and thus takes up 19% of the decay heat. Ba-137m is a decay product of Cs-137 that emits 0.661 MeV of gamma rays and occupies 10% of the heat. The radionuclide that committed the most to the decay heat was Pr-144. Pr-144 is one of the high-yield fission products and mostly becomes Nd-144 by emitting 2.997 MeV of beta energy. Its half-life is short (17.29 minutes), but because of its exceptionally high decay energy, it dominates the decay heat in the short term. But its portion is significantly reduced to 5.48% at 5 years after the discharge, primarily replaced by Y-90 and Ba-137m.

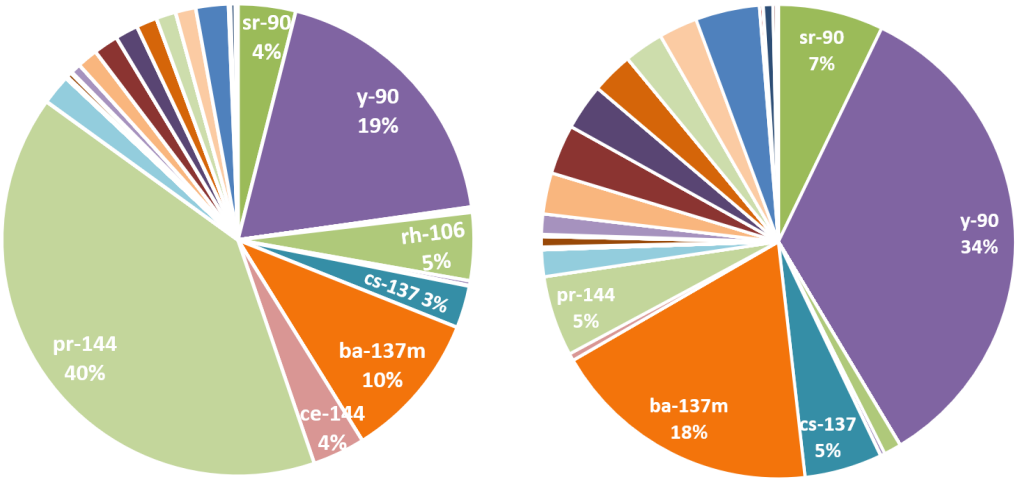

Figure 5-18. Portions of decay heat production 2 years (left) and 5 years (right) after discharge.

5.2 Dose Rate Analysis

In this section, the contact and 30-cm dose rates from a single irradiated fuel container and the storage array of 36 containers are calculated. The storage system supposed here is a hexagonal array of 36 cylindrical fuel salt packages whose H/D ratio is 3. They are not bounded by a container material but surrounded by a vacuum so that it produces the most conservative result. The spacing between them are 8 cm. It is assumed that 5 years have passed since fuel discharge. The neutron and gamma spectrum obtained from the ORIGEN module in the SCALE suite of codes in Section 5.1 will be utilized as the source sampling probabilities in MCNP, as shown in Figure 5-3.

Figure 5-19. Gamma and neutron spectrum 5 years after discharge.

The dose rate from a single container was estimated in order to understand the dose rate when the salt containers are treated one by one. In this case, only one container has served as the radiation source. Together with this case, the dose rate from all 36 containers were simulated for various positions in the container lattice. Two points (Point 2-1 and Point 2-2 in Figure 5-4) were designated where the maximum dose is expected to occur. Referring to those two points, the contact and distant (30 cm) doses, both in axial and radial directions, were estimated. For each of the six (x,y) coordinates described in Figure 5-4, the point tallies were set up for z=H/2 and for z=H (H=height of the salt container), thus 12 tally points were used in this calculation.

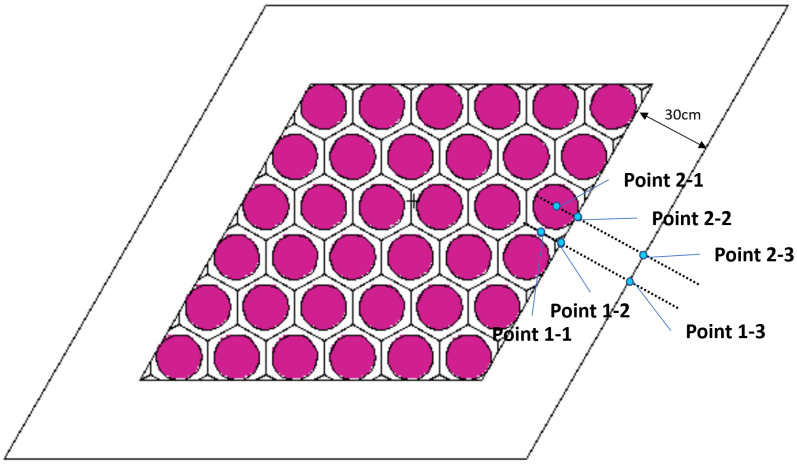

Figure 5-20. Description of the points where neutron and gamma dose will be measured.

5.2.1 Neutron Dose Rate

Using the input parameters discussed above, the dose rates from neutrons were calculated for various tally points. The dose rates per particle, tally errors, and the dose rates from all particles were tabulated in Table 5-2. Note that the total dose rate was obtained by multiplying the source strength per container and the number of containers with the dose rate per particle. That is:

Table 5-13. Neutron dose rates at various points.

Point	Z (cm)	Dose Rate (rem/hr·neutron)	Tally Error	Total Dose Rate (rem/hr)
1-3	H/2	1.90E-10	0.002	1.34E-05
1-2	H/2	1.89E-10	0.0052	1.33E-05
2-3	H/2	1.75E-10	0.0021	1.23E-05
1-3	H+0.0001	6.20E-11	0.0024	4.37E-06
2-3	H+0.0001	5.65E-11	0.0025	3.98E-06
2-2	H/2	5.28E-11	0.0455	3.73E-06
1-1	H+0.0001	5.06E-11	0.0109	3.57E-06
2-1	H+30	2.94E-11	0.0042	2.08E-06
1-2	H	2.82E-11	0.0087	1.99E-06
1-1	H+30	2.69E-11	0.0043	1.89E-06
2-1	H+0.0001	1.16E-11	0.0816	8.18E-07
2-2	H	4.06E-12	0.1902	2.87E-07
Single tank,	H/2	1.05E-10	0.0027	2.06E-07

radially distant				
Single tank, distant	H+0.0001	3.23E-11	0.0031	6.34E-08
Single tank, radially contact	H/2	2.77E-11	0.0737	5.42E-08
Single tank, axially distant	H+30	9.61E-12	0.0068	1.88E-08
Single tank, axially contact	H+0.0001	2.57E-12	0.1117	5.04E-09
Single tank, radially contact	H	9.75E-13	0.0664	1.91E-09

Table 5-2 shows the calculation results in a decreasing order dose rate. The dose rate was the highest at Point 1-3 at z=H/2, recording about 13.4 , closely followed by Point 1-2 at z=H/2. This implies that the receival of neutrons is the highest between two containers, rather than directly facing one container. The differences in the dose rates between other points were almost negligible. As the maximum amount of dose rate from neutrons is well below the amount of radiation dose that Americans receive on average (or),[13] neutrons will not be considered in this storage system's shielding requirements.

Most of the tallies had small tally errors less than 1%. But for some tallies that were close to the container's surfaces showed high relative errors, ranging from 6.64 to 19.02% (light gray in Table 5-2). The reason for the errors is not clear, as the number of histories ran by MCNP was sufficiently large as 10^8. The very close distance between the contact tallies and the container surfaces is suspected to be causing the error. Thus, these results should not be included in our discussions or in developing the shielding requirements.

5.2.2 Gamma Dose Rate

Like in Section 5.2.1, the dose rates from gamma rays were calculated for various tally points. The dose rates per particle, tally errors, and the dose rates from all particles are organized in Table 5-3. The total dose rates were estimated using the following relation. Note that the source strength is significantly larger than neutrons.

Table 5-14. Gamma dose rates at various points.

Point	Z (cm)	Dose Rate (rem/hr·photon)	Tally Error	Total Dose Rate (rem/hr)
1-3	H/2	5.32E-13	0.0042	1149.51
2-3	H/2	4.61E-13	0.0015	996.34
1-2	H/2	3.15E-13	0.0047	681.41
1-3	H+0.0001	1.71E-13	0.0024	370.20
2-3	H+0.0001	1.39E-13	0.0027	299.98
Single tank, radially distant	H/2	4.24E-12	0.0007	254.65
2-2	H/2	6.49E-14	0.052	140.29
2-1	H+30	3.26E-14	0.0032	70.47
1-2	H	3.06E-14	0.006	66.19
1-1	H+0.0001	3.05E-14	0.0095	65.96
1-1	H+30	1.62E-14	0.0069	34.95

Single tank, radially contact	H/2	5.74E-13	0.0236	34.45
Single tank, radially distant	H	5.72E-13	0.0027	34.33
2-2	H	6.28E-15	0.0769	13.57
2-1	H+0.0001	5.86E-15	0.0684	12.67
Single tank, axially distant	H+30	1.12E-14	0.0075	0.67
Single tank, radially contact	H	3.19E-15	0.0909	0.19
Single tank, axially contact	H+0.0001	3.06E-15	0.1025	0.18

As the gamma flux is much higher than the neutron flux, the dose rates were significantly higher for gamma rays. Table 5-3 shows the calculation results in a decreasing order of dose rate. The dose rate was highest at Point 1-3 at z=H/2, recording almost 1,150 rem/hr, followed by Point 2-3 at z=H/2. This implies that the receival of gamma rays is highest between two containers, rather than directly facing one container.

Regardless of the (x,y) points, the dose rate at z=H/2 and radially 30 cm away from the container's surface resulted in the highest dose rate. Obviously, the dose from 36 containers was higher than that from a single container. However, the dose rate from a single container at z=H/2 and radially 30 cm away from the container's surface was 254.65 rem/hr, which is still very high. These dose rates imply that proper shielding is required during the handling and storage of this material.

Again, most of the tallies had small tally errors less than 1%, except for some tallies that were close to the container's surfaces that showed high relative errors, ranging from 5.2 to 10.25% (light gray in Table 5-3). The reason is not clear here either, as the number of histories ran by MCNP was sufficiently large as 10^8. The very close distance between the contact tallies and the container surfaces is suspected to be causing the error. Thus, these results should not be included in our discussions or in developing the shielding requirements.

In conclusion, this data indicates that the dormancy period be at least longer than 5 years after the fuel is discharged to the drain tanks given the amount of decay heat. Together, proper shielding of the containers and the vault walls should be applied as the amount of gamma dose from the bare salts is extremely high. In order to transfer the fuel salts from the drain tanks to the containers, they must be handled with remote-handling equipment that can withstand a high radiation dose.

6. IMPLICATIONS FOR A CHLORIDE-BASED SALT SYSTEM

All the proposed irradiated fuel management processes and the calculations for criticality, decay heat and dose rates were based on the MSRE data, which was a fluoride-based system. In contrast, the reactor that will be demonstrated at the LOTUS testbed is a molten chloride fast reactor. Thus, the requirements and challenges will differ from those of MSRE. This section will investigate the differences in requirements for managing the irradiated fuel salts of fluoride- and chloride-based salt reactors based on a comprehensive literature study on the salt chemistry, material characteristics, postirradiation behavior, neutronics, and the thermal hydraulics and heat removal.

6.1 Salt Chemistry

The salt corrosion chemistry is especially important for MSRs, since the molten halide salts create a harsh environment for the reactor system and thus affect the long-term performance of structural materials. Moreover, the contaminants caused by the ingress of water or oxygen and the neutron

irradiation can make the salt even more oxidizing. Thus, the differences in corrosion chemistry of fluoride- and chloride-based salts were reviewed.

Other than the corrosion issue, there exists another serious challengs called “intergranular cracking (IGC).” It is induced by the diffusion of tellurium (Te), one of the fission products.[14] The preferential diffusion of Te along the grain boundaries creates brittle intermetallic compounds and corrosion products in some Ni-based alloys. Therefore, the metallic material used to construct the primary circuit of an MSR must be compatible with the fuel salt corrosion chemistry.

Fluoride-based Salts

Molten fluorides are highly thermodynamically and radiolytically stable salts. The heat of formation () with Group I–IV elements and transition metals are more negative than , which means that the fluorides are chemically stable. This has been proven at the postirradiation examination of MSRE. It turned out that the molten fluoride salts did not cause much corrosion with the structural metals (which was Hastelloy N), implying that the fertile and fissile fluorides are stable enough not to react with the container alloys.[15]

The major contaminant inducing the corrosion of metals in contact with fluoride-based salts is water. Water reacts with halide ions and forms hydrogen fluoride (HF) or hydrogen chloride (HCl) gases. But this reaction is thermodynamically more favorable for fluorine ions, and the HF gas formed from this is very corrosive and unstable.

The corrosion behavior of various structural metals in contact with the fluoride salts have been investigated, and corrosion-resistant alloys have been developed accordingly throughout history. During those developments, some key factors influencing the corrosion in molten fluorides have been identified.[16]

- First, oxidants in the salt, such as the fuel component UF_4, structural metal impurities, and water impurities could greatly enhance the corrosion of structural metals.[17],[18],[19]
- Second, the Te-induced intergranular cracking. At MSRE, only Te was present in the brittle grain boundary of the Hastelloy N in a high concentration, implying that the cracking is severe enough to form brittle intermetallic compound.[20]
- Third, the temperature gradient formed within the molten coolant salts could be a significant driver for corrosion. Since the equilibrium concentrations of dissolved metal cations are dependent on temperature, the long-term corrosion would be more persistent at the hotter region. But as the thermal-gradient-driven corrosion is inevitable in an MSR circuit, the corrosion rate hot sections must be minimized to prevent the clogging problems at cold sections, especially for heat exchangers.[21]
- Fourth, radiations interact with the corrosion process to cause further damage to the alloys. There are mainly two types of radiations known to cause significant damage:
    - One is neutron radiation. Either by the direct displacement of atoms through collisions with fast neutrons or an absorption of thermal neutrons, vacancies, and interstitials are made inside the alloys, developing point defects in a local area.[22]
    - The other one is helium radiation. This has been observed directly at the Hastelloy N in contact with molten FLiNaK salt. The metals suffered a more severe IGC attack and had many small cavities in the grain matrix.[23] That’s because the radiation-induced surface cavities increase the contact surface area with molten salt, and the corrosion cavities can nucleate from the radiation-induced defects, combining with helium bubbles to grow. These mechanisms and observations imply that radiation could have a significant impact on the corrosion behavior.
- Finally, the corrosion rate and the resistance to Te-induced IGC are subject to alloying elements and their grain size. Some alloy constituents, such as Cr, Nb, Ti, Al, Y, Mo, helped build resistance to embrittlement and IGC.[24],[25],[26] Also, grain refining activities facilitated the diffusion of impurities, inducing higher corrosion rates.[27]

Chloride-Based Salts

Like fluoride-based salts, the oxidant impurities are the biggest factor of corrosion in molten chlorides too. However, the corrosion forms are quite different. While bare metals corrode in a fluoride environment, oxide corrosion products are typically formed on the metal surface in molten chloride salts. Moreover, the formed oxide layers on the structural metals are porous and non-passivating, which is a favorable environment for oxidation.[28],[29],[30] Thus, using the same structural metal, the chloride-based salts may lead to more severe corrosion than fluoride-based ones.

Water, oxygen gas, chlorine gas, metallic cations, and fission products are potential oxidants that significantly influence the corrosion in molten chlorides. The alloying elements composing the structural metal are also important. While a small composition of aluminum (Al) and titanium (Ti) increases the resistance to corrosion by helping the formation of stable oxides that inhibits metal dissolution, carbon (C) and molybdenum (Mo) contents increased the corrosion rates. Chromium (Cr) had a dual role in the alloy corrosion: it could help form protective oxide layers but also facilitate the selective dissolution of less noble Cr from the alloys, increasing the corrosion rate. Previous studies have found out that the optimal Cr content range was 7–22 wt%.[31]

Not only there are deficiencies in the study of the corrosion chemistry of molten chloride salts but also the preparative chemistry methods to produce a high-purity chloride salts for corrosion studies should be developed.[32]

6.2 Material Characteristics

Previous studies have investigated the material characteristics of various fluoride- and chloride-based salts. The major material characteristics that affect the operational performance of an MSR are the melting point, heat capacity, density, viscosity, thermal conductivity, etc. Such thermodynamic properties at an MSR operating temperature (around 700) have been reviewed for various fluoride salts (FLiNaK, NaF-ZrF_4, LiF-NaF-ZrF_4) and chloride salts (LiCl-KCl, NaCl-$MgCl_2$, KCl-$MgCl_2$) by D. F. Williams.[32] Also, Sohar et al. collected an engineering database of liquid salts, including FLiBe.[19] Key results are organized in Table 6-1.

Table 6-15. Material characteristics of typical fluoride- and chloride-based salts.[19],[32]

Class	Salt	Melting Point ()	Heat-Transfer Properties at 700			
			Density (g/cm^3)	Viscosity (cP)	Thermal conductivity ()	Volumetric Heat Capacity ()
Fluoride	LiF-BeF2 (FLiBe)	460	1.94	5.6	1.00	1.09
	LiF-NaF-KF (FLiNaK)	454	2.02	2.9	0.92	0.91
	NaF-ZrF4	500	3.14	5.1	0.49	0.88
	LiF-NaF-ZrF4	436	2.92	6.9	0.53	0.86
Chloride	LiCl-KCl	355	1.52	1.15	0.42	0.43
	NaCl-MgCl2	445	1.68	1.36	0.50	0.44
	KCl-MgCl2	426	1.66	1.40	0.40	0.46

Melting Point

The melting points of salts vary not only on the types of materials included in the salt but also on the weight fractions of each material. Thus, a general comparison between the melting points of fluoride- and chloride-based salts seems unreasonable.

Density

The densities of fluoride salts are generally higher than those of chloride salts, especially for the ones containing Zr. With a fixed mass of fuel salt, using fluoride salt as a carrier salt may reduce the whole salt

volume inside the reactor, coolant system, or storage containers. Thus, fluoride salts are expected to make the system more compact than chloride salts.

Viscosity

The fluoride salts are generally more viscous than chloride salts. A high viscosity is not a desirable characteristic in terms of heat transfer. Plus, viscous salts challenge the removal of residual salts from the reactor core or drain tanks during the defueling or decontamination processes. In this regard, such processes could be easier for chloride-based systems.

Thermal Conductivity

Fluoride- and chloride-based salts show similar thermal conductivities ranging from 0.40 to 0.53 , except for FLiBe and FLiNaK salts. Both salts had thermal conductivities close to unity, which is almost the twice of that of the coolant water under pressurized-water reactor operating conditions. Since only the FLiBe and FLiNaK salts showed exceptionally high thermal conductivities, it would be undesirable to make a general comparison of thermal conductivities between the fluoride- and chloride-based salts.

Volumetric Heat Capacity

The volumetric heat capacity describes how much heat is required to increase the temperature of a material of unit volume by 1 K. The higher the volumetric heat capacity, the more amount of heat can be retained within a small volume, which is one of the ideal characteristics of a coolant. According to Table 6-1, the volumetric heat capacities of fluoride-based salts are almost the double of those of chloride-based salts. Combining the results of thermal conductivity and volumetric heat capacity comparison, fluoride-based salts, especially FLiBe and FLiNaK salts, seem to perform better in terms of heat transfer.

However, since this study is handling the situation when the reactor has stopped its operation, the focus should be on whether these material characteristics will lubricate or impede the decommissioning process. The high density of fluoride-based salts will reduce the salt volume, making the treatment or transport procedures less complex. On the other hand, their high viscosity may cause the fuel or flush salts to adhere to the reactor vessels, pipes, and other structural materials. During the decontamination process, these residual salts must be scraped off with some chemical techniques, which will further complicate the process and increase the costs.

6.3 Postirradiation Behavior

The postirradiation behavior of fluoride-based salts was well documented from MSRE. Most of the fluoride-based salt contains lithium, which produces tritium by neutron irradiation. If the fuel salts are not isolated adequately, the tritium gases could migrate to the heat exchangers and leak outside, increasing the overall radiation dose from the reactor.[15] Thus, many fluoride-based salts, including the FLiBe salts in MSRE, are enriched with Li-7 to suppress tritium production, because Li-7 produces tritium only by an endothermic reaction with high-energy neutrons. Not only do the salts generate tritium but also fluorine and UF_6 gases. It has been proven from MSRE that the radiolysis of FLiBe salt produced fluorine gases constantly, and the effect is exacerbated when the fuel salts are cooled down to room temperature.

On the other hand, almost no experimental data exist for chloride-based salts. However, the neutron irradiation to Cl-35 generates Cl-36, which is a long-lived fission product whose half-life is about 301,300 years and emits 0.71 MeV of decay energy from beta decay. If the amount of Cl-36 production is similar to the level of fluoride gas production, this would add complexity to the irradiated fuel management of chloride-based fuel salts in the long term. Thus, many companies designing molten chloride reactors are considering the enrichment of Cl-37, but this enrichment technique is immature and costly. The radiolytic decomposition of chloride-based salt is not yet proven by experiment, but its behavior is expected to be similar to that of fluoride-based salts.

In sum, the postirradiation behavior of both salts, such as hazardous gas production, should be similar, but more experimental data should be accumulated for chloride salts.

6.4 Neutronics

To elucidate the neutronics of fluoride- and chloride-based salt reactors, their neutron cross sections were compared for various interactions and spectrums. Clear hierarchies were found between the cross sections of fluorine and chlorine for elastic scattering and radiative capture reactions, referring to the JENDL-4.0 cross-section library data (see Figure 6-1).[33] Since chlorine isotopes have larger elastic scattering cross sections at a fast spectrum, chloride-based salts should be a good carrier salt for fast reactors. The capture cross sections were higher for chloride isotopes at almost all neutron energies, implying that chloride-based salts are more likely to produce a large flux of gamma rays before and after the reactor is shut down. If the fluoride-based system changes into a chloride-based one, the radioactivity of the irradiated fuel salt may be increased.

According to Wei et al., from a parametric study of thermal MSR neutronics behavior, the criticality of the reactor depended on the type of fissile isotopes, geometry, and moderator size, rather than whether the salt is a fluoride-based or chloride-based one.[34] Combining the observations from the cross-section data and the results of previous studies, the neutronics between the two salts are not expected to be disparate. However, the level of gamma radiation could be higher for chloride-based salts, possibly requiring a longer dormancy period and decay heat control.

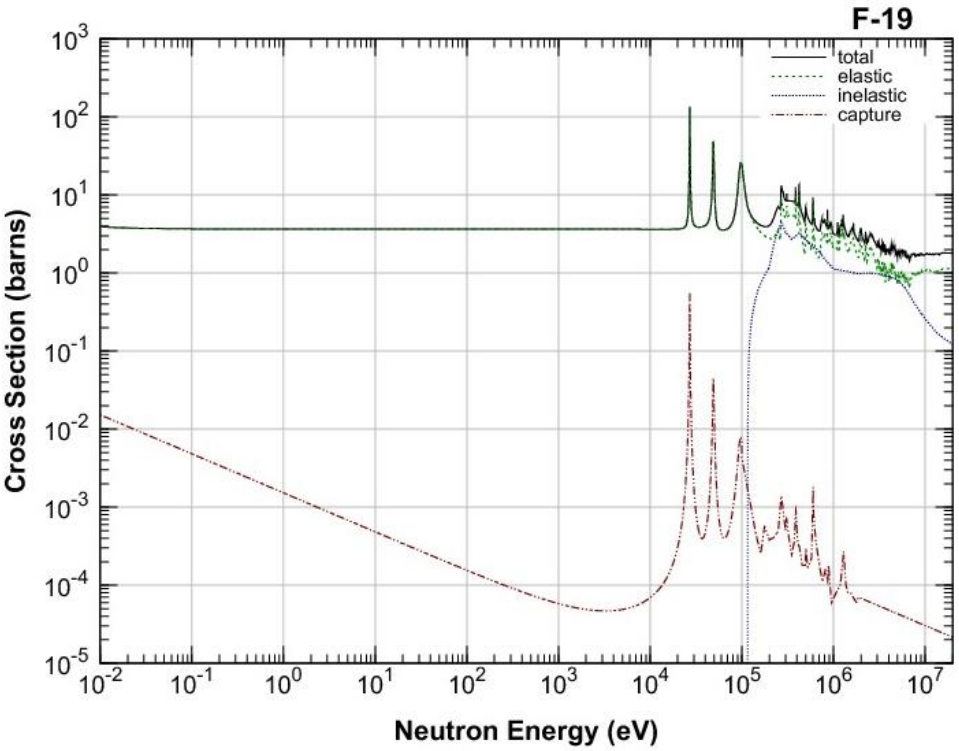
F-19
total
elastic
inelastic
capture
Cross Section (barns)
Neutron Energy (eV)
10^3
10^2
10^1
10^0
10^-1
10^-2
10^-3
10^-4
10^-5
10^-2
10^-1
10^0
10^1
10^2
10^3
10^4
10^5
10^6
10^7

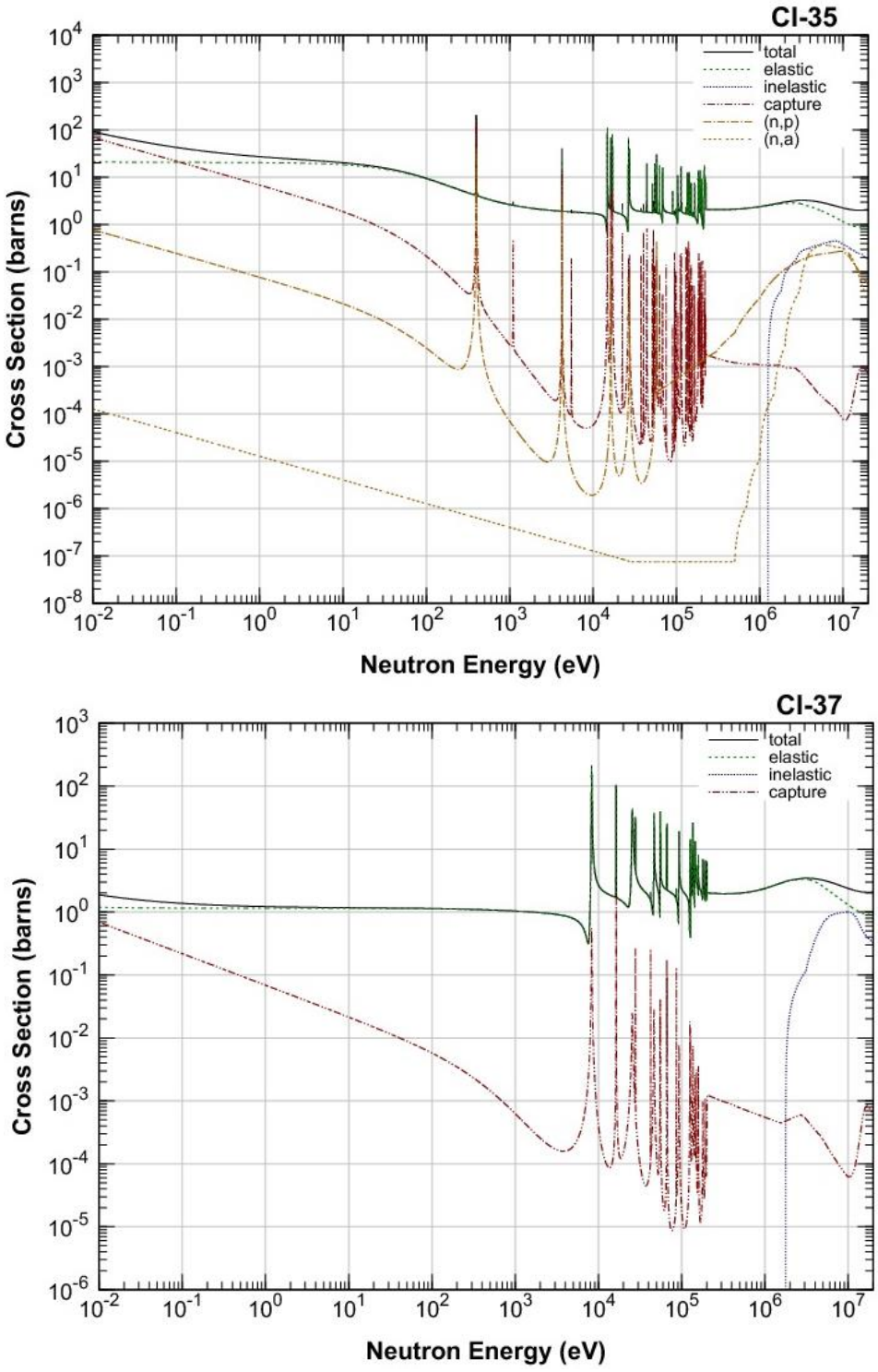

Figure 6-21. Major neutron cross sections of F-19, Cl-35, and Cl-37 (from top to bottom).[33]

6.5 Thermal Hydraulics and Heat Removal

In 2006, D.F. Williams assessed the candidate molten salt coolants for nuclear systems.[32] The key thermal properties of eight fluoride- and chloride-based salts were analyzed candidates. As a result, the FLiNaK salt was the best in terms of turbulent-forced-convection heat-transfer performance. Surprisingly, all fluoride salts had a better heat-transfer performance compared to the chloride salts, and there was not a great deal of difference in heat-transfer performance among the different chloride salt options. Among the chloride salts, LiCl-KCl-$MgCl_2$ was recommended as the best compromise between raw material cost, performance, and melting point. But it should be noted that this study had focused purely on the heat-transfer performances, without any chemical or neutronics consideration.

7. CONCLUSIONS

The goal of this study was to understand the system requirements to use the LOTUS test bed for a molten chloride fast reactor by performing systems analyses and preconceptual development of a storage container for the irradiated fuel salts. The historic MSRE has served as the main reference source for this research. In Section 2, the operational history, lesson learned, and status of MSRE were reviewed, and the challenges of managing irradiated fuel salts from molten fluoride salt reactors were discussed.

Given the challenges presented in Section 2, the irradiated fuel management process of an MSR and the high-level requirements of each step were proposed in Section 3. The irradiated salt treatment process consisted of multiple radioisotope separation stages, which adds complexity to the overall process but reduces the HLW volumes. If pursued, the proposed management process may require the development of additional salt treatment and storage capabilities.

In Section 4, the geometry, number, and spacing between the irradiated fuel salt storage containers were determined from a criticality safety perspective under conservative off-nominal scenarios, such as water ingress and interaction between the containers. To maintain criticality safety under these conditions, the fuel salts should be divided into at least 36 cylindrical containers, whose H/D ratios and spacings should be over 3 and 7 cm, respectively. The criticality search over a wide range of spacings and container geometry under water ingress scenarios indicated that merely increasing the H/D ratio cannot ensure a criticality safety, and thus maintaining a sufficient spacing between the containers with the aid of an engineering spacer grid would be desirable.

In Section 5.1, the decay heat produced from the fuel salt drain tanks were calculated using the ORIGEN module in the SCALE suite of codes. This was also based on the end-of-life composition of the MSRE's irradiated fuel salts. It was recommended that at least 5 years of dormancy is required to drop the level of heat under 100 W/m^3. Subsequently in Section 5.2, the dose rates at the surface of the salt storage system 5 years after fuel discharge were evaluated using MCNP. The gamma dose dominated the whole dose rates, and the maximum dose that could be received from the surface of this storage system was almost 1,150 rem/hr, given that no shielding materials are enclosing the containers or the storage vaults. This value is expected to serve as a basis for establishing the shielding and handling requirements of the storage containers.

Lastly, the differences in the requirements for decommissioning the fluoride- and chloride-based salt reactors were investigated based on a comprehensive literature study. With the same structural metal used, the chloride-based salts may lead to more severe corrosion than fluoride-based ones. Regarding long-term waste management, some undesirable radioisotopes (gaseous tritium and long-lived Cl-36) are produced from both fluoride- and chloride-based salts. Based on the neutron cross-section comparisons, chloride-based salts are more likely to produce a large flux of gamma rays before and after the reactor is shut down. All fluoride salts had a better heat-transfer performance compared to the chloride salts, with FLiNaK showing exceptional heat-transfer capabilities. But there was not a great deal of difference in heat-transfer performance among the different chloride salt options. However, as the experimental data for chloride-based salts are scarce, these deductions must be verified by further investigations and experiments.

REFERENCES

[1] Gizmodo. 2021. “Bill Gate's TerraPower Will Build Experimental Nuclear Reactor in Idaho.” https://gizmodo.com/bill-gates-s-terrapower-will-build-experimental-nuclear-1848112911.

[2] F. J. Peretz. 1996. “Identification and Evaluation of Alternatives for the Disposition of Fluoride Fuel and Flush Salts from the Molten Salt Reactor Experiment at Oak Ridge National Laboratory.” ORNL/ER-380, Oak Ridge National Laboratory. https://doi.org/10.2172/441122.

[3] Jacobs EM Team. 1998. “Record of Decision for Interim Action to Remove Fuel and Flush Salts from the Molten Salt Reactor Experiment Facility at the Oak Ridge National Laboratory.” DOE/OR/02-1671&D2, U.S. Department of Energy Office of Environmental Management.

[4] ORNL, “Cleanup Progress,” Annual Report to the Oak Ridge Regional Community, p. 17, 2020. http://ucor.com/wp-content/uploads/2021/07/CleanProg2020.pdf.

[5] T. M. Eric Abelquist. 2021. “Decommissioning Challenges at the Molten Salt Reactor Experiment Site.” in 2021 Virtual Molten Salt Reactor Workshop.

[6] B. J. Riley, J. McFarlane, G. D. DelCul, J. D. Vienna, C. I. Contescu, C. W. Forsberg. 2019. “Molten salt reactor waste and effluent management strategies: A review.” Nuclear Engineering and Design 345: 94-109. https://doi.org/10.1016/j.nucengdes.2019.02.002.

[7] J. R. Hightower and J. R. Trabalka. 2000. “Depleted Uranium Storage and Disposal Trade Study: Summary Report.” ORNL/TM-2000/10, Oak Ridge National Laboratory. https://doi.org/10.2172/752983.

[8] American Nuclear Society. 2017. “Validation of Neutron Transport Methods for Nuclear Criticality Safety Calculations”. ANSI/ANS-8.24-2017.

[9] J. L. Alwin, F. B. Brown, and M. E. Rising. 2017. “Using Whisper to Support Nuclear Criticality Safety Validation ANSI/ANS-8.24 Requirements and Recommendations.” LA-UR-17-22018, Los Alamos National Laboratory.

[10] D. Shen, M. Fratoni, G. Ilas, and J. Powers. 2006. “Molten salt reactor experiment (MSRE) zero-power first critical experiment with U235,” Nuclear Energy Agency.

[11] National Institute of Standards and Technology. “Atomic Weights and Isotopic Compositions for All Elements.” https://physics.nist.gov/cgi-bin/Compositions/stand_alone.pl?ele=&all=all&ascii=html.

[12] D. F. Williams, G. D. Del Cul, and L. M. Toth. 1996. “A Descriptive Model of the Molten Salt Reactor Experiment After Shutdown: Review of FY 1995 Progress.” ORNL/TM-13142, Oak Ridge National Laboratory. https://doi.org/10.2172/230260.

[13] U.S. NRC. “Doses in Our Daily Lives.” Last updated May 13, 2021. https://www.nrc.gov/about-nrc/radiation/around-us/doses-daily-lives.html.

[14] Y. Jia, H. Cheng, J. Qui, F. Han, Y. Zou, Z. Li, X. Zhou, and H. Xu. 2013. “Effect of temperature on diffusion behavior of Te into nickel.” Journal of Nuclear Materials 441(1–3): 372–379. https://doi.org/10.1016/j.jnucmat.2013.06.025.

[15] D. Holcomb. 2017. “Module 3: Overview of Fuel and Coolant Salt Chemistry and Thermal Hydraulics,” Oak Ridge National Laboratory, November 7–8, 2017, Washington D.C.

[16] S. Guo, J. Zhang, W. Wu, and W. Zhou. 2018. “Corrosion in the molten fluoride and chloride salts and materials development for nuclear applications.” Progress in Materials Science 97: 448–487. https://doi.org/10.1016/j.pmatsci.2018.05.003.

[17] J. W. Koger, "Effect of FeF2 addition on mass transfer in a Hastelloy N - LiF-BeF4-UF4 thermal convection loop system," ORNL, 1972.

[18] F.-Y. Ouyang, C.-H. Chang, B.-C. You, T.-K. Yeh, and J.-J. Kai. 2013. "Effect of moisture on corrosion of Ni-based alloys in molten alkali fluoride FLiNaK salt environments." Journal of Nuclear Materials 437(1–3): 201–207. https://doi.org/10.1016/j.jnucmat.2013.02.021.

[19] M. S. Sohal, A. M. Ebner, P. Sabharwall, and P. Sharpe. 2010. "Engineering Database Liquid Salt Thermophysical and Thermochemical Properties." INL/EXT-10-18297, Idaho National Laboratory. https://doi.org/10.2172/1086824.

[20] H. E. McCoy. 1978. "Status of materials development for molten salt reactors." ORNL/TM-5920, Oak Ridge National Laboratory. https://doi.org/10.2172/5195742.

[21] J. W. Koger. 1973. "Evaluation of Hastelloy N alloys after nine years exposure to both a molten fluoride salt and air at temperatures from 700 to 560C," Oak Ridge National Laboratory.

[22] M. A. Stopher. 2017. "The effects of neutron radiation on nickel-based alloys." Materials Science and Technology 33(5) 518–536. https://doi.org/10.1080/02670836.2016.1187334.

[23] H. Zhu, Z. Wang, M. Cui, B. Li, X. Gao, J. Sun, C. Yao, K. Wei, T. Shen, L. Pang, Y. Zhu, Y. Li, J. Wang, and E. Xie. 2015. "Temperature dependent surface modification of T91 steel under 3.25 MeV Fe-ion implantation," Applied Surface Science 326: 1–6. https://doi.org/10.1016/j.apsusc.2014.11.029.

[24] J. W. Koger. 1972. "Alloy compatibility with LiF--BeF2 salts containing ThF4 and UF4," ORNUTM-4286, Oak Ridge National Laboratory. https://doi.org/10.2172/4381831.

[25] A. K. Misra and J. D. Whittenberger, "Fluoride Salts and Container Materials for Thermal Energy Storage Applications in the Temperature Range 973 – 1400 K," Philadelphia, Pennsylvania, 1987.

[26] C. S. Sona, B. D. Gajbhiye, P. V. Hule, A. W. Patwardhan, C. S. Mathpati, A. Borgohain and N. K. Maheshwari. 2014. "High temperature corrosion studies in molten salt-FLiNaK." Corrosion Engineering, Science and Technology 49(4): 287–295. https://doi.org/10.1179/1743278213Y.0000000135.

[27] L. C. Olson, J. W. Ambrosek, K. Sridharan, M. H. Anderson, and T. R. Allen. 2009. "Materials corrosion in molten LiF–NaF–KF salt." Journal of Fluorine Chemistry 130(1): 67–73. https://doi.org/10.1016/j.jfluchem.2008.05.008.

[28] A. R. Shankar, A. Kanagasundar, and U. K. Mudali. 2012. "Corrosion of Nickel-Containing Alloys in Molten LiCl-KCl Medium." 69(1): 48–57. https://doi.org/10.5006/0627.

[29] J. E. Indacochea, J. L. Smith, K. R. Litko, E. J. Karell, and A. G. Raraz. 2001. "High-Temperature Oxidation and Corrosion of Structural Materials in Molten Chlorides." Oxidation of Metals 55(1–2): 1–16. https://doi.org/10.1023/A:1010333407304.

[30] A. R. Shankar, S. Mathiya, K. Thyagarajan, and U. K. Mudali. 2010. "Corrosion and microstructure correlation in molten LiCl-KCl medium." Metallurgical and Materials Transactions A: Physical Metallurgy and Materials Science 41(7): 1815–1825. https://doi.org/10.1007/s11661-010-0223-5.

[31] K. Vignarooban, P. Pugazhendi, C. Tucker, D. Gervasio, and A. M. Kannan. 2014. "Corrosion resistance of Hastelloys in molten metal-chloride heat-transfer fluids for concentrating solar power applications." Solar Energy 103: 62–69. https://doi.org/10.1016/j.solener.2014.02.002.

[32] D. F. Williams. 2006. "Assessment of Candidate Molten Salt Coolants for the NGNP/NHI Heat-Transfer Loop." ORNL/TM-2006/69, Oak Ridge National Laboratory. https://doi.org/10.2172/1360677.

[33] Japanese Atomic Energy Agency Nuclear Data Center. “Cross-Section library of JENDL-4.0.” https://wwwndc.jaea.go.jp/NuC/index.html.

[34] H. Wei, Y.-T. Chen,. K.-C. Lan, and J. Chen. 2018. “Parametric study of thermal molten salt reactor neutronics criticality behavior.” Progress in Nuclear Energy 108: 409–418. https://doi.org/10.1016/j.pnucene.2018.06.017.